eprints@whiterose.ac.uk
https://eprints.whiterose.ac.uk/

1   **Short title:** Importance of Complex I for the photoperiod response

2

3   **Corresponding author:** Dr Bertrand Gakière, bertrand.gakiere@u-psud.fr

4

5   Institute of Plant Sciences Paris-Saclay (IPS2), CNRS, INRA, Univ. Paris-Sud, Univ. Evry,

6   Univ. Paris-Diderot, Université Paris-Saclay, Bâtiment 630, 91405 Orsay, France

7

8

9   **Article title:** Photoperiod affects the phenotype of mitochondrial complex I mutants

10

11   **Authors names and affiliations:**

12   Pierre Pétriacq[ai], Linda de Bont[a], Lucie Genestout[a2], Jingfang Hao[a], Constance Laureau[b], Igor

13   Florez-Sarasa[c3], Touami Rzigui[b4], Guillaume Queval[a], Françoise Gilard[d], Caroline Mauve[d],

14   Florence Guérard[d], Marlène Lamothe-Sibold[d], Jessica Marion[e], Chantal Fresneau[b], Spencer

15   Brown[e], Antoine Danon[a5], Anja Krieger-Liszkay[f], Richard Berthomé[g], Miquel Ribas-Carbo[c],

16   Guillaume Tcherkez[h], Gabriel Cornic[b], Bernard Pineau[a6], Bertrand Gakière[ad1], Rosine De

17   Paepe[a].

18

19   a. Institute of Plant Sciences Paris-Saclay (IPS2), CNRS, INRA, Univ. Paris-Sud, Univ. Evry,

20   Univ. Paris-Diderot, Université Paris-Saclay, Bâtiment 630, 91405 Orsay, France

21   b. Ecologie, Systématique et Evolution, Univ. Paris-Sud, CNRS, Université Paris-Saclay,

22   Bâtiment 362, 91405 Orsay Cedex, France

23   c. Grup de Recerca en Biologia de les Plantes en Condicions Mediterranies, Departament de

24   Biologia, Universitat de les Illes Balears, Palma de Mallorca, Spain

25   d. Plateforme Métabolisme Métabolome, Institute of Plant Sciences Paris-Saclay IPS2,

26   CNRS, INRA, Univ. Paris-Sud, Univ. Evry, Univ. Paris-Diderot, Université Paris-Saclay,

27   Bâtiment 630, 91405 Orsay, France

28   e. Institute for Integrative Biology of the Cell (I2BC), CNRS, CEA, Univ. Paris-Sud,

29   Université Paris-Saclay, Campus de de Gif, CNRS, Avenue de la terrasse, 91190 Gif-sur-

30   Yvette Cedex, France

31   f. Institute for Integrative Biology of the Cell (I2BC), CNRS, CEA, Univ. Paris-Sud,

32   Université Paris-Saclay, Campus de Saclay, CEA Saclay, 91191 Gif-sur-Yvette cedex, France

33   g. Laboratoire des Interactions Plantes Micro-organismes (LIPM), UMR INRA 441/CNRS

34   2594, CS 52627, 31326 CASTANET TOLOSAN CEDEX, France

1

35   h. Research School of Biology, ANU College of Medicine, Biology and Environment,

36   Australian National University, 2601 Canberra ACT, Australia

37   i. *bi*OMICS Facility, Department of Animal and Plant Sciences, The University of Sheffield,

38   Sheffield, UK

39

40   **One sentence summary**

41   Respiratory complex I mutants do not properly acclimate to long day conditions in

42   Arabidopsis, demonstrating the importance of mitochondria for the photoperiod response

43

44   **Footnotes**:

45   **1. Authors' contributions**

46   R.D.P. conceived the original screening and research plans; B.G., G.T., R.B and G.C.

47   supervised the experiments; P.P., B.G., L.G., P.B., L.dB., JF.H, I.F-S. C.L., G.Q, J.M, T.R.,

48   C.F, A.K-L performed most of the experiments; F.G., C.M. provided technical assistance;

49   M.R-B, G.T. designed the experiments and analyzed the data; R.D.P. conceived the project

50   and wrote the article with contributions of all the authors; B.G., G.C. and GT. supervised and

51   complemented the writing.

52

53   **2. Funding information**

60

61   **3. Present addresses of authors**

62   1. The author responsible for distribution of materials integral to the findings presented in this

63   article in accordance with the policy described in the Instructions for Authors

64   (www.plantphys.org) is: Dr Bertrand Gakière, bertrand.gakiere@u-psud.fr

65   2. Current address: LABOGENA, Domaine de Vilvert, 78352 Jouy-en-Josas CEDEX, France

66   3. Current address: Central Metabolism Group, Molecular Physiology Department, Max

67   Planck Institute of Molecular Plant Physiology, Am Mühlenberg 1, 14476 Potsdam-Golm,

68   Deutschland

69   4. Current address: Institut Sylvo-Pastorale (I. S. P. Tabarka) BP n 345, 8110 Tabarka,

70   Tunisie

71   5. Current address: LBMCE, UMR 8226, Sorbonne Universités; UPMC Université Paris 06,

72   Centre National de la Recherche Scientifique, Institut de Biologie Physico-Chimique, 75005

73   Paris, France

74   6. Deceased

75

76

77   *Abstract*

78

79   Plant mutants for genes encoding subunits of mitochondrial Complex I (CI,

80   NADH:ubiquinone oxidoreductase), the first enzyme of the respiratory chain, display various

81   phenotypes depending on growth conditions. Here, we examined the impact of photoperiod, a

82   major environmental factor controlling plant development, on two *Arabidopsis thaliana* CI

83   mutants: a new insertion mutant interrupted in both *ndufs8.1* and *ndufs8.2* genes encoding the

84   NDUFS8 subunit, and the previously characterized *ndufs4* CI mutant. In long day (LD)

85   condition, both *ndufs8.1* and *ndufs8.2* single mutants were indistinguishable from Col-0 at

86   phenotypic and biochemical levels, whereas the *ndufs8.1 ndufs8.2* double mutant was devoid

87   of detectable holo-CI assembly/activity, showed higher AOX content/activity and displayed a

88   growth-retardation phenotype similar to that of the *ndufs4* mutant. Although growth was more

89   affected in *ndufs4* than *ndufs8.1 ndufs8.2* under short day (SD) condition, both mutants

90   displayed a similar impairment of growth acceleration after transfer to LD as compared to the

91   WT. Untargeted and targeted metabolomics showed that overall metabolism was less

92   responsive to the SD-to-LD transition in mutants than in the WT. The typical LD acclimation

93   of carbon, nitrogen-assimilation and redox-related parameters was not observed in *ndufs8.1*

94   *ndufs8*. Similarly, NAD(H) content, that was higher in SD condition in both mutants than in

95   Col-0, did not adjust under LD. We propose that altered redox homeostasis and NAD(H)

96   content/redox state control the phenotype of Complex I mutants and photoperiod acclimation

97   in Arabidopsis.

98

99

100   **Introduction**

101

102   Complex I (CI, NADH:ubiquinone oxidoreductase, EC 1.6.5.3), the first enzyme of the

103   respiratory chain of most Eukaryotes, including plants, couples electron transfer to proton

104   translocation through the inner mitochondrial membrane (Klodmann et al., 2010). CI is a L-

105   shaped multimeric enzyme of around 1 MDa in size, composed of a matrix-faced peripheral

106   arm carrying the NADH-oxidizing activity (N module), a connecting module (Q module

107   transferring electrons to the quinone-binding site), and a hydrophobic intra-membrane arm

108   carrying the proton translocation activity (P module). Eukaryotic CI comprises more than 40

109   subunits, of which 14 are also present in the ancestral bacterial enzyme (core subunits,

110   Efremov et al., 2010). They are encoded by either mitochondrial (mt) genes (*e.g. NAD*) or by

111   nuclear genes that might be present in multiple copies (see Table 1 in Meyer et al., 2011).

112   Mutations in both mitochondrial and nuclear genes have been characterized in various plant

113   species. Mutants devoid of NAD subunits were characterized in maize (*ncs2,* deleted for

114   *NAD4*, Marienfeld and Newton, 1994) and in *Nicotiana* (*N.*) *sylvestris* CMSI and CMSII,

115   deleted for *NAD7*, Pla et al., 1995). Mutations in genes controlling *NAD* cis/trans processing

116   have been described in *N. sylvestris,* maize and *Arabidopsis thaliana* (Arabidopsis) (review

117   by Colas des Francs-Small and Small, 2014), and insertion mutants lacking nuclear encoded

118   subunits have been characterized in Arabidopsis (Meyer et al., 2009; Kühn et al., 2015; Soto

119   et al., 2015). Impaired holo-complex assembly/activity are common features of all plant

120   mutants characterized so far, but putative intermediate assembly forms have been observed in

121   several cases (Gutierres et al., 1997; Karpova and Newton, 1999; Perales et al., 2005; Pineau

122   et al., 2008; Meyer et al., 2009, 2011; Kühn et al., 2015). A general respiratory impairment,

123   measured as either O_2 consumption of leaf disks or CO_2 emission by attached leaves in the

124   dark (dark respiration) has not been observed, and *in organello* experiments showed induction

125   of non-phosphorylating NAD(P)H dehydrogenases (Rasmusson et al., 2008) in all cases

126   analyzed (Sabar et al., 2000; Marienfeld and Newton, 1994; Meyer et al., 2009; Keren et al.,

127   2012). Furthermore, both the capacity of the alternative oxidase (AOX) pathway, which

128   bypasses the cytochrome oxidase (COX) pathway, and the AOX protein content were

129   increased in all mutants.

130   Plant CI mutants have various phenotypes, from mild to severe or even near-lethal

131   (Kühn et al., 2015): in addition to a slow-growing phenotype, morphological distortions and

132   male sterility were reported in maize *NCS2* (Karpova and Newton, 1999) and in *N. sylvestris*

133   NMS1 and CMSII (De Paepe et al., 1990). Seedlings of Arabidopsis *nMat1, 4* (Keren et al.,

134   2012, Cohen et al., 2014) and *ndufv1* (Kühn et al., 2015) mutants barely survive unless grown

135   *in vitro* with sucrose supplementation. Differential impact of the mutations was also observed

136   at physiological and metabolic levels. Decreased photosynthetic activity is not a general effect

137   and was reported in the *N. sylvestris* CMSII and NMS1 mutants (Sabar et al., 2000; Dutilleul

138   et al., 2003a; Priault et al., 2007) and in the Arabidopsis *ca2 cal2* mutant only (Soto et al.,

139   2015). In the *N. sylvestris* mutants, limited carbon supply resulting from higher

140   photorespiration is likely to contribute to the slow-growth phenotype (Priault et al., 2006b).

141   Although similar metabolic alterations were observed in *N. sylvestris* (Dutilleul et al., 2005;

142   Szal et al., 2008; Djebbar et al., 2012) and Arabidopsis CI mutants (Meyer et al., 2009; Keren

143   et al., 2012), as increased levels of amino acids, ATP and NAD(H), noteworthy differences

144   were recently reported between Arabidopsis mutants (Kühn et al., 2015). Moreover, an

145   increase in total reactive oxygen species (ROS) content was reported for many Arabidopsis CI

146   mutants (Meyer et al., 2009; Keren et al., 2012; Soto et al., 2015), but not in the CMSII

147   mutant (Dutilleul et al., 2003b). The reasons for these inconsistencies are presently unknown.

148   Complementation studies, performed for CMSII (Pineau et al., 2005), *opt43* (de Longevialle

149   et al., 2007), *ndufs4* (Meyer et al., 2009) and for mutants in *CA2/CAL2* genes encoding

150   CA/CAL γ-carbonic anhydrase subunits (Sunderhaus et al., 2006, Soto et al., 2015) indicated

151   that additional mutations are not involved in the altered phenotype in these cases. It has been

152   proposed that the presence of traces of holo-CI might attenuate mutant deficiencies (Kühn et

153   al., 2015). Alternatively, it is possible that assembly intermediates might interfere with

154   normal oxidative phosphorylation or have additional functions, as suggested by Keren et al.

155   (2012).

156   The phenotype of several CI mutants is affected by growth conditions. CMSII plants

157   showed altered responses to environmental conditions such as light (Priault et al., 2006a),

158   nitrogen and CO_2 (Pellny et al., 2008; Hager et al., 2010), and were fully male sterile under

159   very low illumination only (De Paepe et al., 1990). They were differentially affected by

160   drought stress (Galle et al., 2010; Djebbar et al., 2012). Also, the growth defect of the

161   Arabidopsis *ca2 cal2* mutant was rescued under non-photorespiratory conditions (Soto et al.,

162   2015). However, despite its importance for plant development and productivity, the

163   photoperiod response in CI mutants has not been investigated yet. Plants can be classified into

164   day neutral (DN), short day (SD) and long day (LD) plants on the basis of the minimum

165   duration of light per day necessary to trigger the transition from a vegetative growth phase to

166   a reproductive state. Arabidopsis is a facultative LD species that blooms earlier in LD (≥ 12h

167   day length) than in SD, and photoperiod affects morphological (leaf thickness, thylakoid

168   organization) and physiological parameters (carbon assimilation-related parameters, stomatal

169   conductance), redox state and stress responses (Robbins and Pharr, 1987; Gibon et al., 2004,

170   2009; Becker et al., 2006; Lepistö and Rintamäki, 2012; Queval et al., 2012). Although it has

171   been reported that day length (16h vs 12h) impacts on the phenotype of the *ABO5* mutant

172   affected in *nad2* splicing (Liu et al., 2010) and that photoperiodic control was altered in *cal*

173   mutants (Wang et al., 2012) Arabidopsis CI mutants have been fully characterized in LD only

174   and a link between CI and photoperiod remain to be studied.

175   Here, we examined the impact of different photoperiod regimes on two different

176   Arabidopsis CI mutants: a new insertion mutant interrupted in both *ndufs8.1* and *ndufs8.2*

177   genes encoding the NDUFS8 subunit belonging to the core CI (Efremov et al., 2010), and the

178   previously characterized *ndufs4* mutant (Meyer et al., 2009; Kühn et al., 2015). Under

179   greenhouse LD condition, both *ndufs8.1* and *ndufs8.2* single mutants were indistinguishable

180   from Col-0 at both biochemical and phenotypic levels. In contrast, the *ndufs8.1 ndufs8.2*

181   double mutant was devoid of holo-CI assembly/activity and displayed a growth-retardation

182   phenotype similar to that of *ndufs4*. Although growth was less affected in *ndufs8.1 ndufs8.2*

183   than in *ndufs4* under SD conditions, both mutants had an impaired growth response when

184   transferred from SD to LD. We further provide insights into metabolomics and biochemical

185   alterations associated with acclimation to LD, and discuss how mitochondrial CI activity

186   might interact with photoperiod acclimation in Arabidopsis.

187

188

189   **Results**

190

191   ***Molecular and biochemical characterization of single and double mutants of the NDUFS8***

192   ***subunit***

193

194   Mutant lines carrying a T-DNA insertion in the *ndufs8.1* (*At1g16700*) and the *ndufs8.2*

195   *(At1g79010)* genes (Col-0 accessions) were obtained from the SALK-institute collection.

196   Both genes are composed of 6 exons (Fig. 1A) and proteins share 94% similarity. By

197   sequencing T-DNA left border insertion PCR products, we localized the insertion sites in the

198   first intron and in the third intron in *ndufs8.1* and *ndufs8.2,* respectively. Knockout mutations

199   were confirmed by PCR and RT-PCR, using *ndufs8.1* and *ndufs8.2* primer combinations: no

200   *ndufs8.1* and *ndufs8.2* transcripts could be detected in the corresponding mutants (Fig. 1B and

201   Fig. 1C). In Col-0 seedlings and leaves, *NDUFS8.2* was found to be about 2.5 times more

202   expressed than *NDUFS8.1* (Fig. 1C). No changes for *NDUFS8.2* transcripts were detected in

203   the *ndufs8.1* mutant, and for *NDUFS8.1* transcripts in the *ndufs8.2* mutant, indicating no

204   adjustment at the gene expression level. The *ndufs8.1 ndufs8.2* double mutant, recovered from

205   crossing single mutants with the *ndufs8.2* mutant used as the male donor, was lacking both

206   *NDUFS8.1* and *NDUFS8.2* transcripts (Fig. 1B, C). In both single and double mutants, DNA

207   and RNA patterns were stably maintained over five selfing generations and all biochemical

208   and physiological analyses were thus performed on S3-S5 offspring.

209   In order to see whether the expression of *ndufs8.1* and *ndufs8* genes was required for

210   CI assembly and activity, leaf proteins were solubilized with digitonin, a detergent preserving

211   the association of respiratory chain super-complexes, in particular I-III$_2$ super-complexes

212   (Pineau et al., 2008), and subjected to BN-PAGE. In-gel NADH dehydrogenase activity,

213   revealed by NDH/NBT staining, was observed around 1 MDa (which corresponds to CI size)

214   in the WT and in *ndufs8.1* and *ndufs8.2* single mutants, but was not detectable in the *ndufs8.1*

215   *ndufs8.2* double mutant (Fig. 2, left). Moreover, a signal around 1,500 kDa corresponding to

216   supercomplex I-III$_2$ (Pineau et al., 2008), was observed in single mutants as in the WT, but

217   not in the double mutant. Similarly, the immunostaining obtained using antiserum directed

218   against NAD9 (mitochondrion-encoded CI subunit located in the peripheral arm, Klodmann

219   et al., 2010) was observed in the WT and single mutants, but not in the double mutant (Fig. 2,

220   middle). By contrast, the antibody directed against the COX2 subunit of cytochrome oxidase

221   (Complex IV) gave a similar signal in all cases (Fig. 2, right). Two-dimensional BN/SDS-
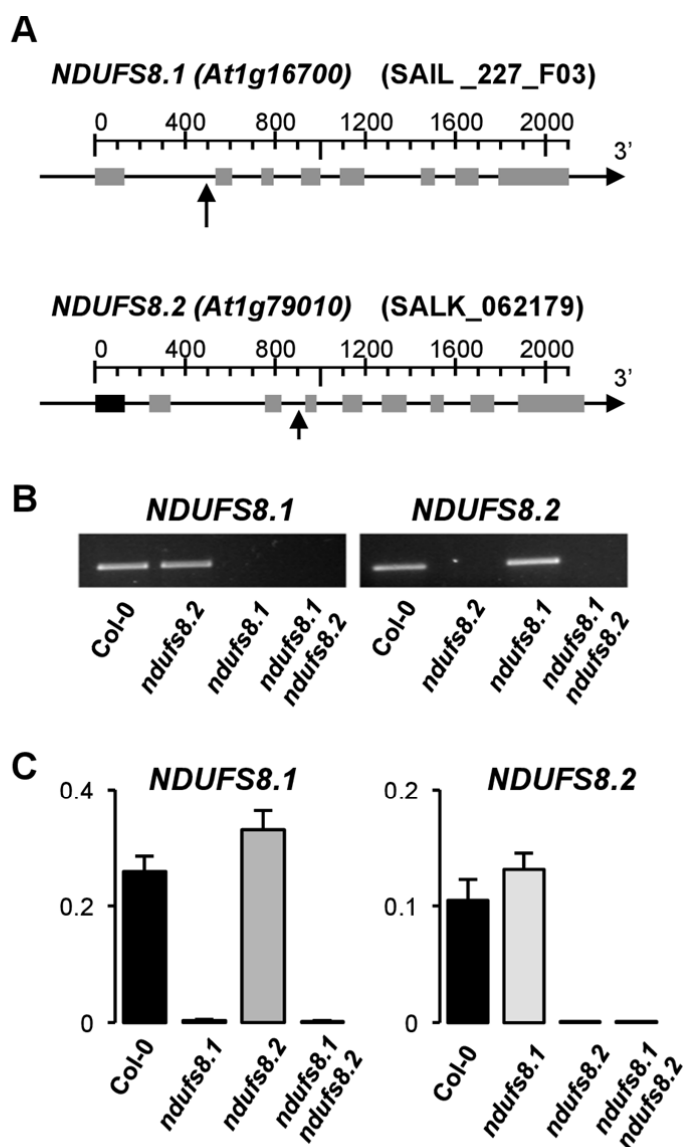
Figure 1. Molecular characterization of single and double insertion mutants affected in the two Arabidopsis genes encoding the NDUFS8 subunit of Complex I

A, gene structure and sites of insertion of T-DNA in *NDUFS8.1* (*At1g79010*) and *NDUFS8.2* (*At1g16700*) genes (arrows). **B**, electrophoresis of RT-PCR products using *NDUFS8.1* and *NDUFS8.2* specific primers in the WT (Col-0), *ndufs8.1* and *ndufs8.2* single mutants, and the *ndufs8.1 ndufs8.2* double mutant. **C,** RT-qPCR analysis of *NDUFS8.1* and *NDUFS8.1* genes in the WT (Col-0), the *ndufs8.1* and *ndufs8.2* single mutants and the *ndufs8.1 ndufs8.2* double mutant, using *ACT2* as a reference. Data are means + SE of 3 independent measurements.

222   PAGE of total root membrane proteins solubilized with β-dodecylmaltoside which dissociates

223   respiratory super-complexes, failed to reveal a clear CI pattern in the double mutant, despite

224   presence of trace amounts of CI subunits (Supplemental Fig. S1). For example, the 76 kDa
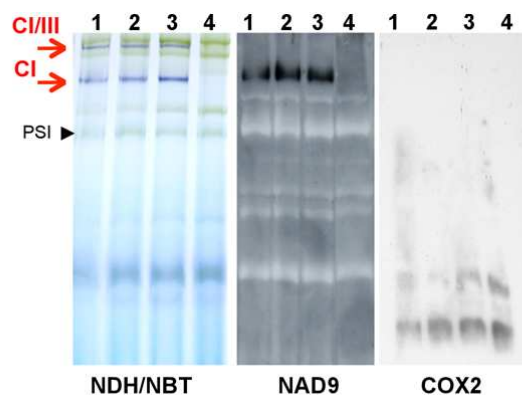
Figure 2. Complex I assembly/activity in Col-0 and single and double mutants for the NDUFS8 subunit

Membrane proteins extracted from leaves of Col-0 (1), single *ndufs8.1* (2), *ndufs8.2* (3) and *ndufs8.1 ndufs8.2* double (4) mutants were solubilized with digitonin that preserves assembly of super-complexes and resolved by BN-PAGE on 4/13% gradient acrylamide gels. After migration, gels were stained for CI activity using NADH/NBT or blotted on PVDF membranes for immuno-detection studies.
- Left: in-gel NADH/NBT-stained leaf proteins; CI and the CI/III super complex (purple signals, red arrows), detected in Col-0 and in both *ndufs8.1*- and *ndufs8.2* single mutants, are absent in the double mutant. PSI originated from thylakoid membranes is indicated by arrowheads (see Pineau et al., 2008).
- Middle: the anti-NAD9 immuno-signal revealed at the level of CI in the WT and in both *ndufs8.1* and *ndufs8.2* single mutants, is not detected in the *ndufs8.1 ndufs8.2* double mutant.
- Right: accumulation of Complex IV using anti-COX2 antibody (bottom of the gel) is similar in all genotypes.

225   subunit, which is part of NADH dehydrogenase module located in the peripheral arm, was

226   hardly distinguishable in the mutant.

227   In spite of impaired CI activity, leaf total oxygen consumption in the dark was

228   similar in *ndufs8.1 ndufs8.2* and Col-0 (v_t, Fig. 3A). The cytochrome vs. AOX partitioning

229   determined using oxygen isotope discrimination (Guy et al., 1989; Ribas-Carbo et al., 1995),

230   showed a slight increase in the O_2 consumption rate by the AOX pathway (v_{alt}) in the mutant.

231   This was associated with a marked increase in AOX capacity (Fig. 3B) and protein content

232   (Fig. 3C). Although the anti-CA2 antibody is partly a-specific, a mitochondrial-specific CA

233   signal was observed in comparable amounts in both mutant and WT (Fig. 3C). Similarly, the

234   signal corresponding to the NAD9 subunit (synthesized inside mitochondria) was found in

235   both genotypes.

236   Hence, these results indicate that, as expected from undetectable levels of

237   *NDUFS8.1* and *NDUFS8.2* transcripts, the NDUFS8 subunit is not synthesized (or only in

238   trace amounts) in the double mutant, resulting in CI mis-assembly. Despite marked

239   disturbances in the composition of respiratory complexes, including accumulation of AOX

240   proteins, no abnormalities of mitochondrial (ultra)structure could be observed by electron

241   microscopy in *ndufs8.1 ndufs8.2* (Supplemental Fig. S2), in contrast to what was observed in

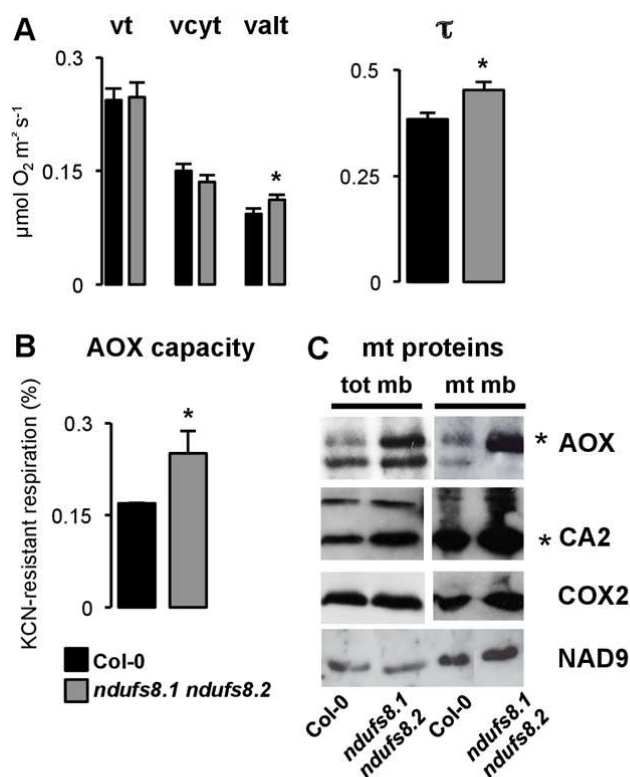242   *nMat* mutants (Keren et al., 2012; Cohen et al., 2014).

Figure 3. Respiratory pathways and mitochondrial proteins in Col-0 and *ndufs8.1 ndufs8.2* mutant

A, Respiration rates of Col-0 and of the *ndufs8.1 ndufs8.2* double mutant were determined by oxygen discrimination. Measurements were performed on plants grown in controlled chambers in 12h/12h, day/night; vt: total oxygen uptake; vcyt: cytochrome oxidase activity; valt: alternative oxidase activity (AOX); τ: partition to the AOX pathway. Data are means +SE of measurements performed on at least 3 different plants; * indicates significant difference between WT and mutant.
B, AOX capacity: % of cyanide resistant respiration in leaf tissues, determined as in Florez-Sarasa et al. (2009). Data are means + SE of measurements performed on at least 3 different plants; * indicates significant difference between Col-0 and mutant.
C, Immunodetection of mitochondrial (mt) proteins on total leaf membranes (tot mb, left) and mitochondrial membranes (mt mb, right). * indicates mitochondrial specific immuno-signals. The experiment was performed at least 3 times with similar results.

243

244 ***Development of single and double mutants for the NDUFS8 subunit under LD condition***

245

246   Under greenhouse conditions (*i.e.* natural illumination, supplemented by 16 h lighting

247 with fluorescent tubes), seedling development, rosette morphology and adult-stage size of

248 *ndufs8.1* and *ndufs8.2* single mutants were similar to the WT (Supplemental Fig. S3). That is,

249 the lack of any of the two NDUFS8 proteins appeared to be fully compensated for at all

250 developmental stages under greenhouse conditions. However, development of *in vitro*

251 germinated seedlings was slightly delayed in both single mutants (Supplemental Fig. S3D).

252   In contrast to single mutants, growth of the *ndufs8.1 ndufs8.2* double mutant was

253   markedly delayed both under greenhouse and growth chamber (16h/8h, day/night, at 100

254   µmol m^{-2} s^{-1} PAR) conditions. Reduced development of *in vitro* germinating seedlings could

255   be partly alleviated by sucrose supplementation, as previously reported for other Arabidopsis

256   CI mutants (Keren et al., 2012; Kühn et al., 2015). Leaves were somewhat more round-shaped

257   in *ndufs8.1 ndufs8.2* than Col-0 ones, although not otherwise malformed. Bolting was delayed

258   for about 2 weeks, whereas leaf size at the mature rosette stage, height and leaf dimensions of

259   adult plants, structure of the inflorescence, flower morphology and number of siliques were

260   unaffected (Supplemental Fig. S3B). Pollen was fully fertile, as tested by Alexander dye

261   staining (Supplemental Fig. S3C). At both rosette and adult stages, dimensions and aspect of

262   *ndufs4* plants were similar to those of *ndufs8.1 ndufs8.2* ones, despite a lower germination

263   rate (Supplemental Fig. 3C) and a slightly lower growth rate of young plantlets (Supplemental

264   Fig. S4B). Taken together, and considering the absence of phenotypic alterations in single

265   mutants, these observations provide compelling evidence that the slow-growth phenotype of

266   *ndufs8.1 ndufs8.2* double mutant is caused by the high reduction in CI activity.

267

268   ***Growth enhancement associated to the transfer from SD to LD condition is similarly***

269   ***compromised in both* ndufs8.1 ndufs8.2 *and* ndufs4 *mutants***

270

271   To determine how the photoperiod regime influenced the slow-growth phenotype

272   when CI is deficient, *ndufs8.1 ndufs8.2* and *ndufs4* mutants were grown in controlled

273   chambers (100 µmol m^{-2} s^{-1} PAR) in SD condition (8h/16h, day/night) up to the 8-9 leaf stage

274   (stage referred to as SD0 thereafter), and then either transferred to LD (16h/8h) or maintained

275   in SD under same light intensities. In what follows, 'LD-plants' and 'SD-plants' refer to

276   plants that were transferred to LD or maintained under SD, respectively. The number of days

277   after the transition is denoted as SD3 and LD3 (after 3 days), SD6 and LD6 (after 6 days), and

278   so on.

279   Surprisingly (and in marked contrast to LD condition, see Supplemental S3), *ndufs4*

280   plants grew less rapidly than *ndufs8.1 ndufs8.2* plants in SD condition (Supplemental Fig.

281   S4). Young rosette plants were more compact in *ndufs4* than in the two other genotypes, and

282   necrotic points could be seen in some long term SD grown plants (inset in Supplemental Fig.

283   S4A).

284   However, despite their developmental difference, the growth acceleration of *ndufs8.1*

285   *ndufs8.2* and *ndufs4* plants following their transfer to LD was similarly lower than in Col-0
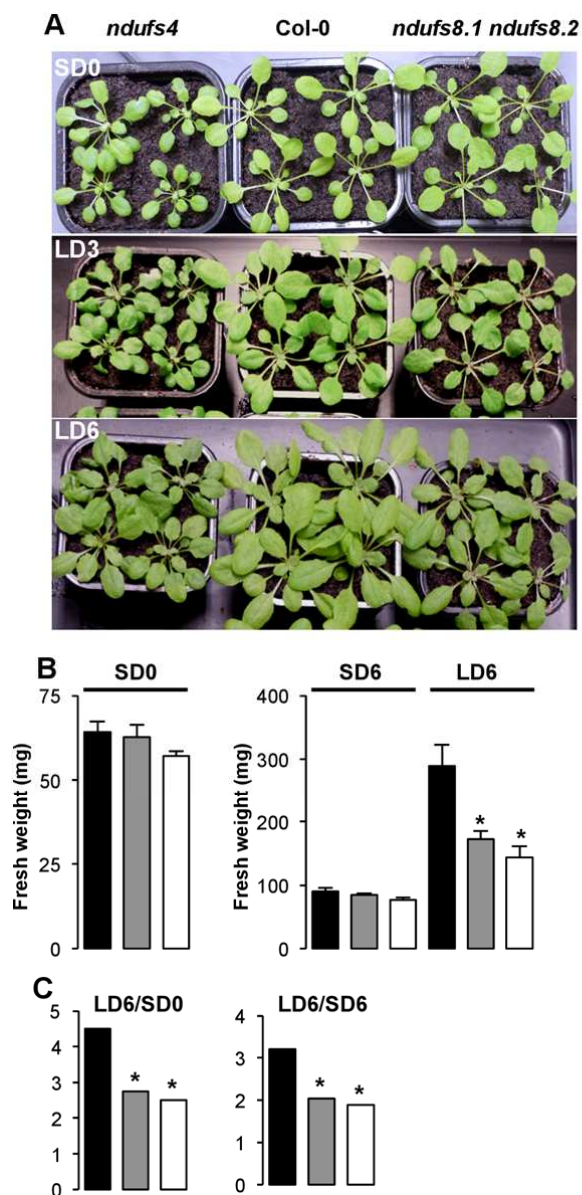
Figure 4. Growth comparisons of Col-0, *ndufs8.1 ndufs8.2* and *ndufs4* plants in the short day (SD) to long day (LD) transfer experiment

A, Col-0 and mutant plants (*ndufs8.1 ndufs8.2* and *ndufs4*) were initially grown in controlled rooms under SD to achieve a similar development (8-9 leaf state, SD0), then transferred to LD for 3 days (LD3) or 6 days (LD6).
B, Histograms of fresh weight (FW, mg) of SD0, SD6 and LD6 plants in Col-0 (black), *ndufs8.1 ndufs8.2* (grey) and *ndufs4* (white). Data are means +SE of measurements on at least 8 different plants in all genotypes. Differences between mutant and Col-0 values are much higher in LD than in SD condition; * indicate significant differences between mutants and Col-0 according to Student t test.
C, LD/SD ratios of plant biomass (FW) in Col-0 (black), *ndufs8.1 ndufs8.2* (grey) and *ndufs4* (white) plants; asterisks indicate significant differences between mutants and Col-0.

286   for which enhanced growth under LD was already obvious at day 3 after transfer (Fig. 4A).

287   The LD6-to-SD0 and LD6-to-SD6 ratios of shoot biomass were lower for both mutants as

288   compared to the WT (Fig. 4B). In LD12 plants, the increase in all parameters of mature leaves

289   (shoot biomass, leaf mass area (LMA) and thickness, dimensions of palisade cells) was lower

290 in *ndufs8.1 ndufs8.2* than in Col-0 (Supplemental Fig. S5). Hence, despite the lower growth

291 rate of *ndufs4* under SD condition, the response of both mutants to their transfer to LD

292 condition is similarly impaired as compared to WT. This suggests that the altered photoperiod

293 response of growth is associated with reduced levels of CI activity but not to the absence of a

294 specific CI subunit or another genetic alteration.

295

296 ***Leaf metabolome responds differently to photoperiod in WT,* ndufs8.1 ndufs8.2 *and***

297 **ndufs4 *plants***

298

299   Previous studies in tobacco (Dutilleul et al., 2003b, 2005; Hager et al., 2010) and

300 Arabidopsis CI mutants (Meyer et al., 2009; Keren et al., 2012; Cohen et al., 2014; Kühn et

301 al., 2015) reported alterations in metabolic signature under standard LD conditions, with

302 higher contents in TCA intermediates and amino acids. Here, we compared WT- and mutant

303 metabolic profiles during transfer from SD to LD by untargeted HILIC-qTOF-MS, using

304 leaves sampled at day 6 in the middle of the light cycle. This technique provides a signature

305 of polar metabolites, in particular organic and amino acids, sugars and other metabolites

306 involved in central metabolism (see Supplemental Methods; Paglia et al., 2012; Pétriacq et al.,

307 2016). Accurately detected mass-to-charge (*m/z*) features (error = 0.4 ppm) in negative (ESI⁻,

308 17326 ions) and positive (ESI⁺, 18341 ions) ionization modes were integrated using XCMS

309 (Smith et al., 2006). Resulting ion intensities were subjected to un-supervised principal

310 component analysis (PCA, Fig. 5A) to obtain a metabolic overview between genotypes and

311 photoperiod regimes. PCA showed complete separation of both genotypes and photoperiods

312 in ESI⁻ and ESI⁺. In SD, all three genotypes were rather distinct and *ndufs4* seemed to show

313 the most distinct metabolic phenotype. In LD, while ESI⁻ analysis showed a close grouping of

314 *ndufs8.1 ndufs8.2* with *ndufs4* as compared to WT, ESI⁺ analysis revealed overlapping

315 profiles between the two CI-deficient mutants. Furthermore, untargeted HILIC profiles were

316 poorly impacted by the SD-to-LD transfer in both mutants, especially for ESI⁺ (Fig. 5A).

317 Metabolic relationships between samples were also visualized by hierarchical clustering

318 analysis (HCA) in order to reveal metabolic similarities between genotypes and photoperiod

319 (Fig. 5B). Clearly, both CI mutants were rather similar in LD, and *ndufs4* displayed the

320 greater metabolic variation in SD. Hence, untargeted metabolomics support the outcome of

321 growth analysis: both CI mutants are more similar in LD than in SD (Supplemental Fig. S4

322 and Supplemental Fig. S5) and show limited response to SD-to-LD transfer (Fig. 4).
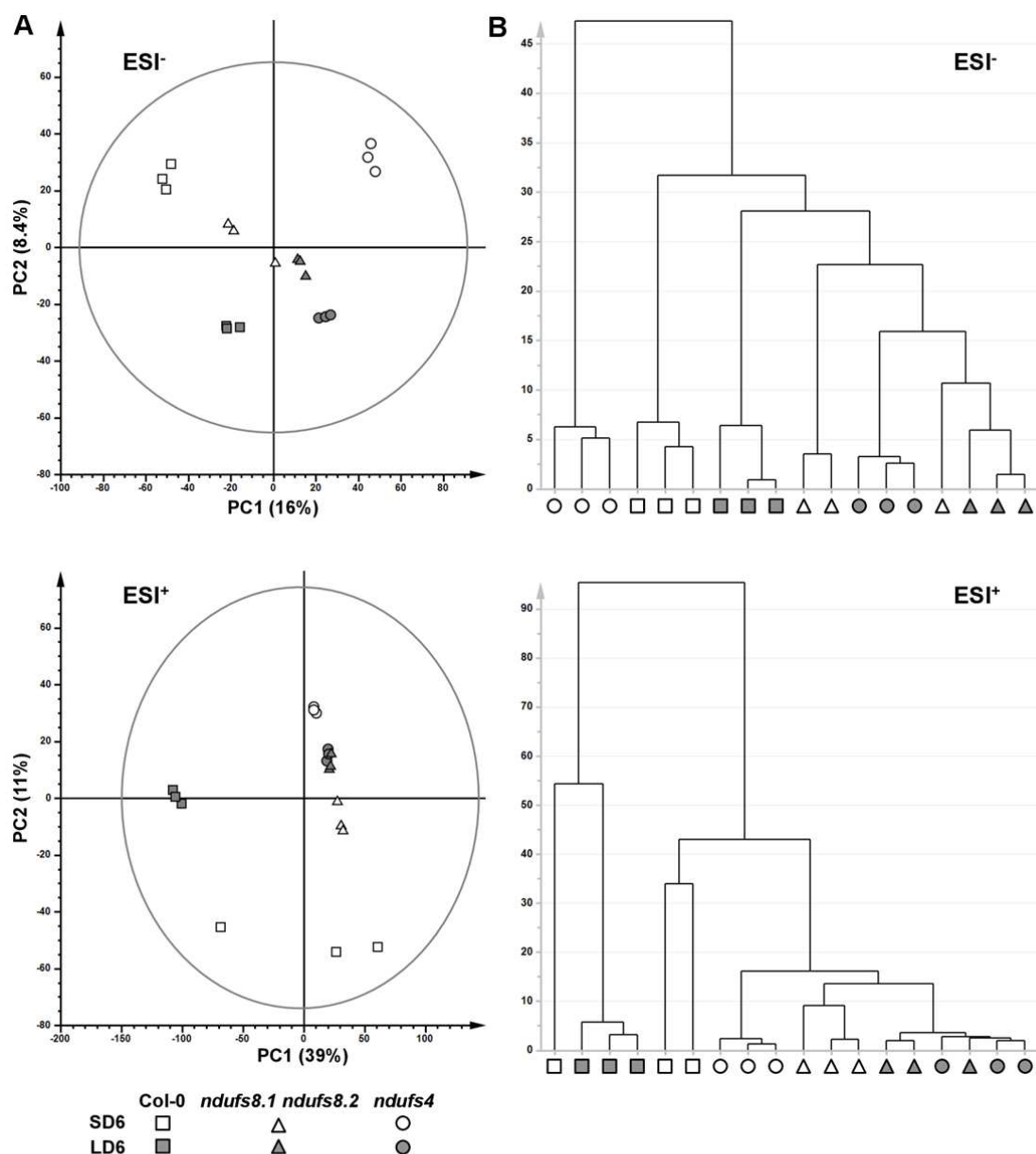
Figure 5. Untargeted metabolomics by HILIC-qTOF-MS

Multivariate analyses of 18341 anions (ESI⁻) and 17326 cations (ESI⁺) detected by HILIC-qTOF-MS from Col-0 (squares), *ndufs8.1 ndufs8.2* (triangles) and *ndufs4* (circles) plants grown in short days (SD, white symbols) or long days (LD, grey symbols) *(n = 3)*.
A, un-supervised principal component analysis (PCA) displaying the overall metabolic trends between samples. Variances are given into brackets.
B, hierarchical clustering analysis (HCA) showing metabolic relationships between genotypes and photoperiod (Single linkage, tree sorted by size).

323   In order to identify metabolites driving the differences in LD acclimation between

324   WT and mutants, we carried out targeted metabolomics by GC-MS at 6 days (SD6 and LD6).

325   In SD, both mutants had elevated contents in TCA intermediates (citrate, succinate, fumarate

326   malate), glycerol-3-phosphate (a redox shuttle metabolite) and most amino acids as compared
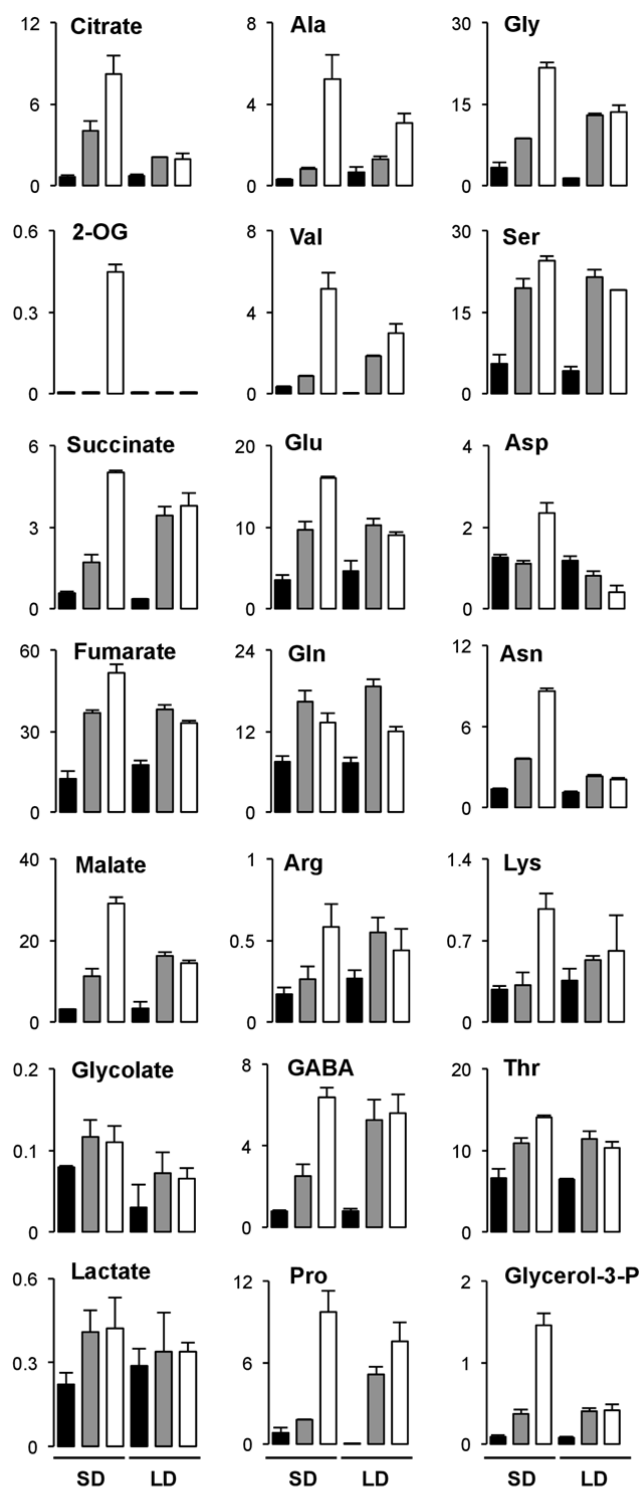
14

Figure 6. GC-MS determination of metabolites in Col-0, *ndufs8.1 ndufs8.2* and *ndufs4* plants
Leaves were sampled from SD6/LD6 plants at the middle of the day period; analyte contents are expressed in relative units; black columns: Col-0; grey columns: *ndufs8.1 ndufs8.2;* white columns: *ndufs4*

327   to the WT (Fig. 6). In most cases, the increase was higher in *ndufs4* than in *ndufs8.1 ndufs8.2*,

328   and 2-OG was detected in *ndufs4* only. While the SD-to-LD transition was associated with a

329   slight increase in succinate and malate and in some amino acids (Ala, Val, Arg, Pro, GABA,

330   Lys) in *ndufs8.1 ndufs8.2,* it induced a decrease in these metabolites in *ndufs4*. As a result,

331   metabolite pools of TCA intermediates and most amino acids were similar and higher than in

332   the WT, in both *ndufs8.1 ndufs8.2* and *ndufs4* under LD. This is consistent with untargeted

333   metabolomics, showing lower metabolic differences between the mutants under LD than

334   under SD (Fig. 5), possibly reflecting their similar growth rates under LD condition

335   (Supplemental Fig. S4).

336   To get precisions on the timing and day-night effect of photoperiod-dependent

337   metabolomics, GC-MS profiling was performed on WT and *ndufs8.1 ndufs8.2* plants at days

338   3 and 6 after transfer, both at the middle of the light period and at the end of the dark period at

339   day 6. 40 metabolites were significantly (ANOVA, $P < 0.01$) affected by the genotype (Fig.

340   7). This included sugars (Glc, Fru), TCA intermediates (citrate, malate, succinate and

341   fumarate) and amino acids (Gly, Ser, Ala, Gln, Glu and Gln), which were in larger amounts in

342   the mutant regardless of the time point considered, the light condition and the photoperiod

343   (see also Supplemental Figs. S7-9). 33 analytes were significantly affected by the

344   photoperiod, partly overlapping with genotype-significant ones (*e.g.* malate, succinate;

345   Supplemental Fig. S10). From a supervised orthogonal partial least-squares-discriminant

346   analysis (OPLS-DA, $R^2 = 0.99$ and $Q^2 = 0.89$) in each genotype, the effect of each feature in

347   explaining the discrimination was quantified using a Volcano plot representing the variable

348   importance for the projection (VIP) against the coefficient along axis 1 (loading score;

349   Supplemental Fig. S11A and Supplemental Fig. S11B). Using ANOVA analysis, 18 analytes

350   were found to be significant for the genotype × photoperiod interaction (Supplemental Fig.

351   S11 C), including hexoses (Glc, Fru), TCA derivatives (succinate, malate, citramalate) and

352   amino acids (Ser, Asn, Glu and Gln). HPLC quantitation of amino acids revealed larger

353   overall differences between *ndufs8.1 ndufs8.2* and Col-0 under LD than under SD

354   (Supplemental Fig. S12). There was a substantial effect of LD on amino acids derived from

355   photorespiration and/or glycolysis (Ser, Gly, Ala, Val, Trp, Leu) and 2-OG (Glu, Gln, Arg,

356   Orn) in the mutant, but a limited effect on oxaloacetate-derived amino acids (Asp, Asn, Thr,

357   Lys, Met).

358   Finally, we examined whether the marked differences in TCA derivatives between

359   WT and *ndufs8.1 ndufs8.2* were associated to changes in transcripts associated with enzymes

360   believed to be rate-limiting steps for the TCA pathway in the light (Tcherkez et al., 2009 and

361   references therein; Araújo et al., 2012). Except for lower 2-oxoglutarate dehydrogenase 2

362   (*OXO2*) and aconitase 3 (*ACO3)* transcripts under SD, and *OXO2* and fumarase (*FUM*)

363   transcripts under LD (Supplemental Fig. S13), little significant differences were observed

364   between WT and mutants. Regarding the photoperiod effect, accumulation of *FUM*
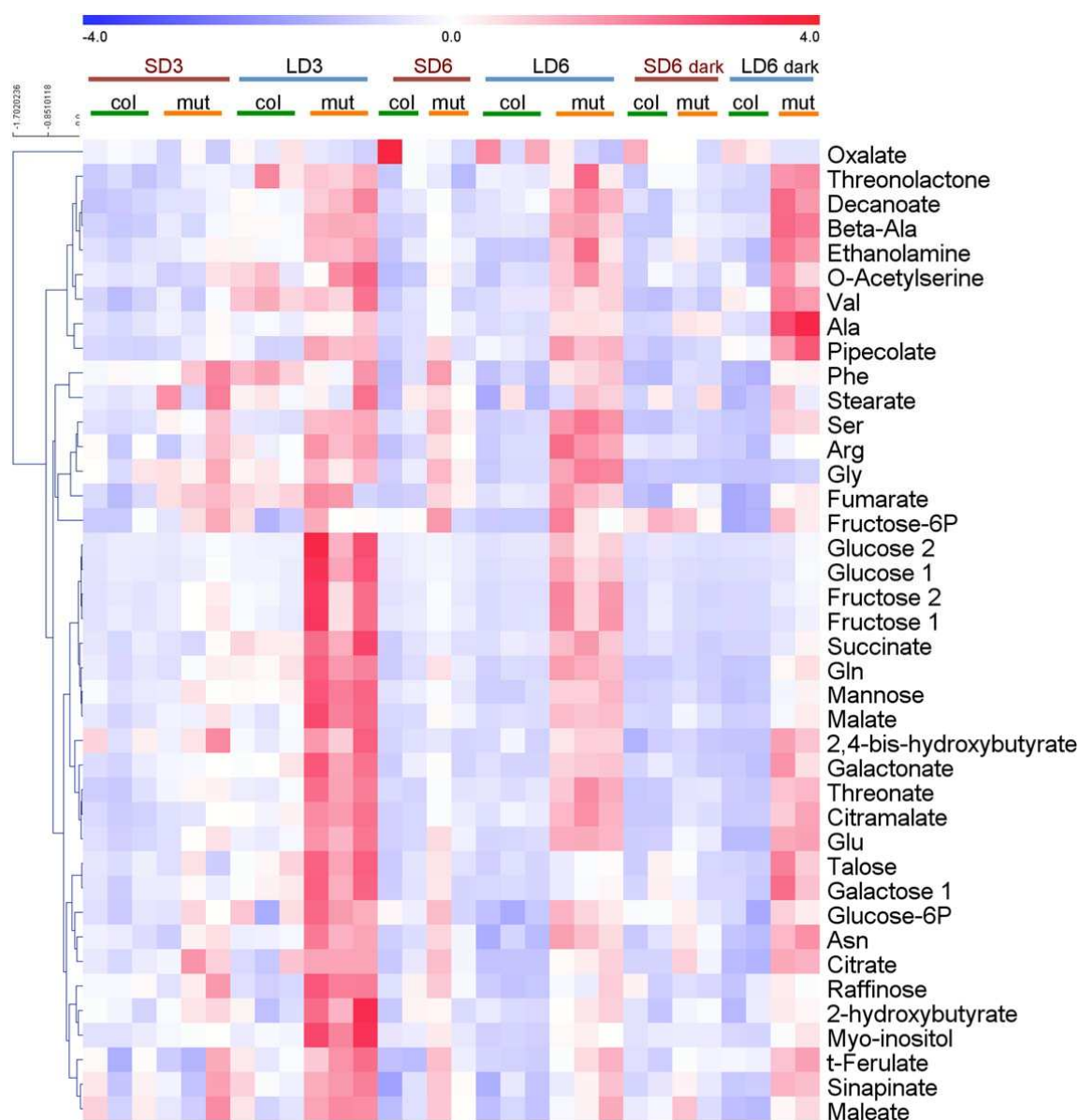
Figure 7. Heat-map and hierarchical clustering (cosine correlation) of metabolites found to be significant with respect to genotype (in a two-way ANOVA GC-MS metabolomics)

Col-0 (col) and *ndufs8.1 ndufs8.2* (mut) leaves were sampled from SD3/LD3 plants at the middle of the light period and from SD6/LD6 plants both at the middle of the light period and at the end of the night period (dark). Metabolomic analyses were carried out 3 times (*i.e.*, 3 biological replicates). Relative metabolite contents are represented as mean-centered values with a color scale (blue, low content; red, high content). Numbers close to metabolite names refer to individual analytes associated with the metabolite of interest.

365   transcripts in LD WT leaves was consistent with that of fumarate. Although a comprehensive

366   study would require an analysis of all transcripts of TCA-related enzymes, these results

367   suggest that the impact of photoperiod on TCA cycle gene expression is reduced in the

368   *ndufs8.1 ndufs8.2* mutant.

369   In summary, our metabolomic analyses (both untargeted HILIC-qTOF-MS and

370   targeted GC-MS) show that, as for growth phenotype (Fig. 4), *ndufs8.1 ndufs8.2* and *ndufs4*

371 display a rather similar metabolic phenotype in LD compared to SD (Fig. 5 and Fig. 6). Also,

372 despite differences in TCA derivatives and some amino acids upon transfer from SD to LD,

373 there is limited metabolic adaptation to LD in both mutants, in agreement with their impaired

374 growth response.

375

376 ***Photoperiod modulates alterations of carbon and nitrogen assimilation-related parameters***

377 ***in the* ndufs8.1 ndufs8.2 *mutant***

378

379   The remodeled metabolomes of CMSII (Sabar et al., 2000; Dutilleul et al., 2003a; Priault

380 et al., 2006a; 2007) and *ndufs4* (Meyer et al., 2009) mutants were associated with alterations

381 in carbon and nitrogen assimilation under LD condition**.** Here, we found that although net

382 CO_2 assimilation (*A*) was lower in the *ndufs8.1 ndufs8.2* mutant than in the WT under

383 elevated light and was stimulated by LD in both genotypes (light response curves shown in

384 Supplemental Fig. S14A), it was similar in all cases at growth PAR (photosynthetic photon

385 flux density, 100 µmol m^{-2} s^{-1} PAR, see inset). Likewise, the response of *A* to intercellular

386 CO_2 mole fraction (*C_i*) at moderate light (300 µmol m^{-2} s^{-1} PAR), and its stimulation by LD

387 condition did not significantly differ between the two genotypes **(**Supplemental Fig. S14B)**.**

388 Interestingly, the relationship between *C_c* (intracellular CO_2 mole fraction at the carboxylation

389 sites) and *C_i* was the same in the two genotypes (Supplemental Fig. S14C), suggesting that

390 internal conductance for CO_2 (dissolution-diffusion) was similar. Also, we did not detect

391 differences in chloroplast number and thylakoid organization (distribution or ultrastructure)

392 between WT and *ndufs8.1 ndufs8.2* (Supplemental Fig. S6) in either LD or SD conditions.

393 Moreover, the electron flux to oxygenation (*J_o*) and leaf glycolate oxidase activity did not

394 significantly differ between genotypes and photoperiods (Supplemental Fig. S14D),

395 indicating a similar photorespiration rate in all cases. Nevertheless, apparent carboxylation

396 efficiency (Ce, the initial slope of the *A/C_i* relationship, inset in Supplemental Fig. S14A),

397 Rubisco capacity and total leaf ATP contents were higher in the mutant than in WT in SD but

398 were not stimulated by LD (Fig. 8A). Also, chlorophyll *a/b* ratio, stomatal conductance (*g_s*)

399 and dark respiration (CO_2 evolution in darkness) did not significantly differ between

400 genotypes in SD and increased in LD in the WT only. Hence, physiological parameters

401 showed that growth impairment in *ndufs8.1 ndufs8.2* did not come from gas exchange

402 alteration (photosynthetic or photorespiratory effects) in either SD or LD but photoperiod

403 acclimation of photosynthetic parameters appeared to be compromised in the mutant.

404   In contrast to carbon assimilation, nitrogen assimilation was markedly affected in the
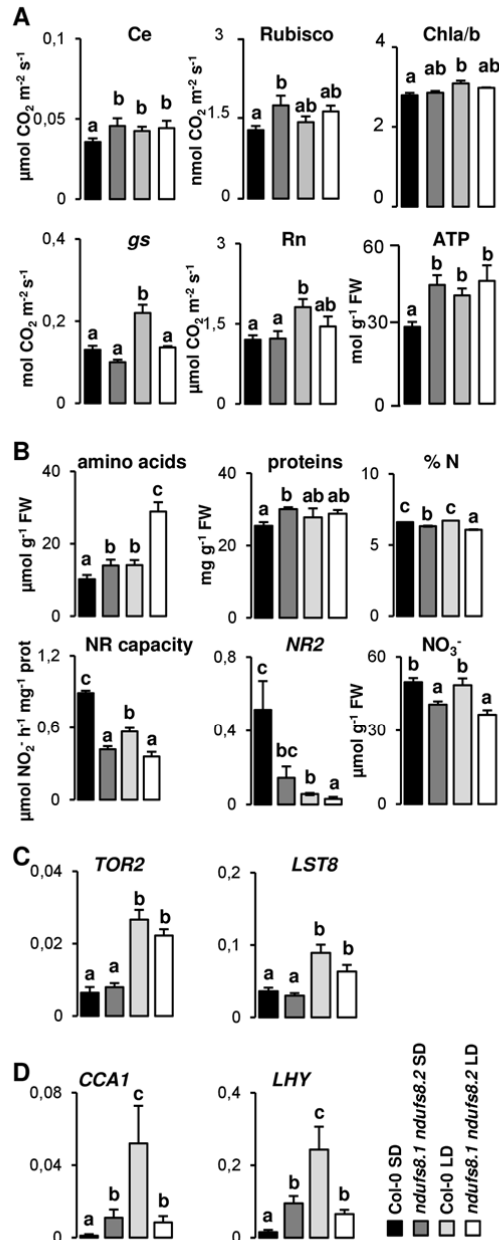
Figure 8. Analysis of growth-related parameters in Col-0 and *ndufs8.1 ndufs8.2*

Leaves were sampled from Col-0 and *ndufs8.1 ndufs8.2* plants at the middle of the light period at the day 12 time point; SD: short day; LD: long day.
A, Carbon exchange-related parameters determined on leaves of 2-3 month old rosette plants at the same developmental stage. Carboxylation efficiency (ce, μmol CO_2 m^{-2} s^{-1}); stomatal conductance for CO_2 (*gs*, mol m^{-2} s^{-1}) calculated at growth illumination; Rubisco capacity (*in vitro* measured maximum activity, nmol CO_2 min^{-1} mg prot^{-1}); chlorophyll a/chlorophyll b ratios; night respiration (Rn, CO_2, μmol CO_2 m^{-2} s^{-1}) and total leaf ATP (nmol g^{-1} FW) are means + SE of 3-6 measurements on different plants. Different letters indicate significant differences according to Student *t* test.
B, Nitrogen assimilation-related parameters. Total leaf free amino acids (μmol g^{-1} FW) determined from HPLC quantification (see Supplemental Figure S12); soluble proteins (mg g^{-1} FW); %N (organic total material, including nitrate) ; NR capacity (maximum activity, μmol NO_2^- h^{-1} mg^{-1} prot); RT-qPCR analysis of the major nitrate reductase gene (*NR2*, relative expression to *ACT2*); nitrate contents (μmol g^{-1} FW). Data are means +SE of 3-6 measurements on different plants. Different letters indicate significant differences according to Student t test.
C, RT-qPCR analysis of *TOR2/LST8* genes of the nutrient-dependent TOR pathway using *ACT2* as a reference. Data are means +SE of 3-6 measurements on different plants. Different letters indicate significant differences according to Student t test.
D, RT-qPCR analysis of *CCA1/LHY* clock regulators.
Data are means +SE of 6 measurements on different plants. Different letters indicate significant differences according to Student t test.

405   *ndufs8.1 ndufs8.2* mutant (Fig. 8B). Despite an increase in the mutant of total amino acids

406   (*i.e.* 20% higher than in the WT under SD and about two fold higher under LD) and proteins

407   contents (under SD), total N content (%) was slightly reduced under both photoperiods (Fig.

408   8B). Moreover, maximum NR activity, transcript levels of the major nitrate reductase gene

409   (*NR2*) and nitrate contents were lower in the mutant than in the WT under SD. Since nitrogen

410   assimilation was not significantly affected by photoperiod in the mutant whereas it was lower

411   in LD than in SD plants in the WT (also observed by Gibon et al., 2009), this resulted in

412   lesser phenotypic differences under LD. In addition, we examined the expression of *TOR2*

413   and *LST8*, two key genes of the TOR pathway, which were previously found to be involved in

414   growth and photoperiod adaptation (Moreau et al., 2012). Both genes were up-regulated in

415   LD as compared to SD in both *ndufs8.1 ndufs8.2* and WT, thus suggesting that the accelerated

416   growth rate in LD might benefit from the TOR pathway independently of CI activity (Fig.

417   8C), although post-transcriptional changes might be involved. We also measured transcript

418   levels of *CCA1* and *LHY* clock regulators, which are important for growth and flowering

419   (reviewed in Nagel and Kay, 2012). Remarkably, levels of both transcripts were significantly

420   higher in the mutant than in the WT under SD, but lower under LD due their stimulation by

421   LD in the WT (Fig. 8D). Although these expression profiles would require a comprehensive

422   analysis of full diurnal cycle and other clock regulators, they suggest that the genetic control

423   of the circadian rhythm might be altered in *ndufs8.1 ndufs8.2* plants. Taken together, results

424   show that carbon and nitrogen metabolisms are less affected by the SD to LD transfer in

425   *ndufs8.1 ndufs8.2* than in the WT, in possible relation to an altered circadian rhythm in the

426   mutant.

427

428   ***Photoperiodic regime differentially modulates redox homeostasis in WT and the* ndufs8.1**

429   **ndufs8.2** *mutant*

430

431   Signaling of the photoperiod response has been proposed to be under redox control in

432   Arabidopsis (Lepistö and Rintamäki, 2012). ROS accumulation has been previously observed

433   in various Arabidopsis CI mutants, including *ndufs4* (Meyer et al., 2009; Keren et al., 2012;

434   Soto et al., 2015), but not in the tobacco CMSII mutant (Dutilleul et al., 2003b). In this work,

435   the high heterogeneity between individual illuminated leaves prevented us from

436   demonstrating any consistent differences in ROS content between *ndufs8.1 ndufs8.2* and WT

437   under both photoperiods, using nitroblue tetrazolium (NBT) and diaminobenzidine (DAB)

438   staining of superoxide and hydrogen peroxide, respectively (Supplemental Fig. S15). We

439   therefore used spin-trapping EPR spectroscopy. A typical EPR comparison of SD and LD

440   plants is shown in Fig. 9A, indicating no difference between WT and mutant illuminated leaf

441   disks (during 60 min) of SD plants. In both genotypes, the ROS content was low after a dark

442   period (60 min), reflecting the absence of photosynthesis. In the WT, the amount of apoplastic
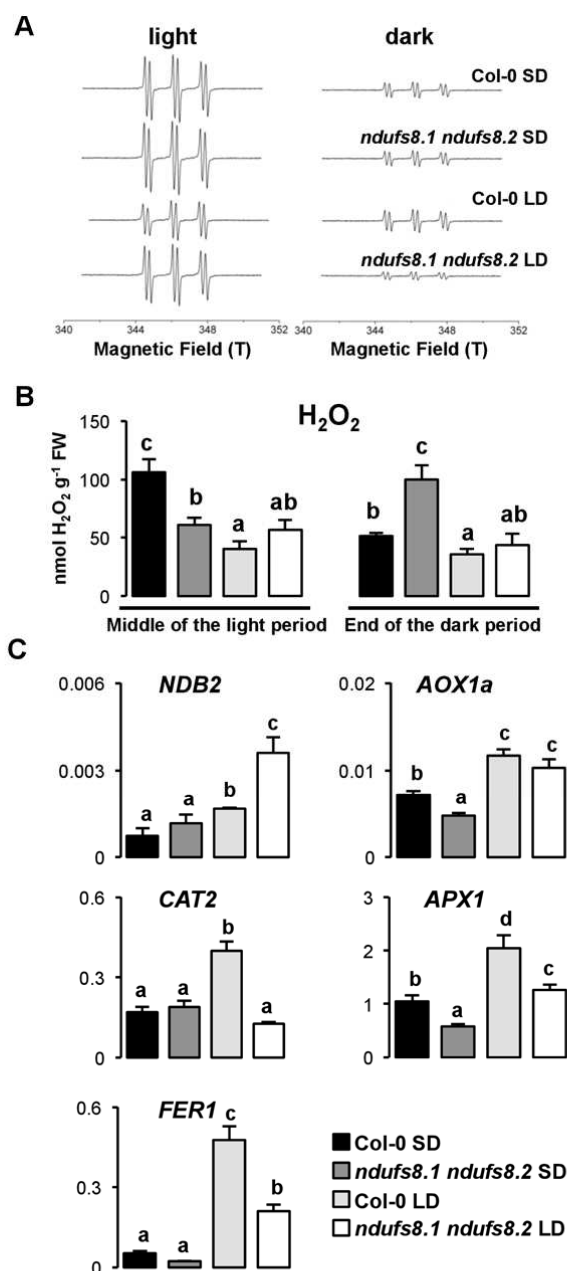
Figure 9. ROS content and expression levels of antioxidant enzymes in Col-0 and *ndufs8.1 ndufs8.2* plants maintained under SD and LD conditions

A, Typical EPR spectroscopy spectra, performed on leaf disks sampled from SD12/LD12 plants, as described in Michelet and Krieger-Liszkay (2012).
B, Total soluble ROS pools (nmol H_2O_2 g^{-1} FW) detected by luminol chemiluminescence in leaves sampled from SD12/LD12 plants at the middle of the light period (left) and at the end of the dark period (right). Data are means +SE of measurements on 4-6 different plants. Different letters indicate significant differences according to Student *t* test.
C, RT-qPCR analysis of redox enzymes of leaves sampled from SD12/LD12 plants at the middle of the light period; *ACT2* was used as a reference. Data are means +SE of measurements on 3-6 different plants. Different letters indicate statistical differences according to Student *t* test.

443 ROS diffusing to the medium was visibly lower in LD than in SD, as previously reported

444 (Michelet and Krieger-Liszkay, 2012). By contrast, there was no clear photoperiod effect on

445 ROS amounts in the *ndufs8.1 ndufs8.2* mutant. We then determined leaf endogenous ROS

446 content using luminol chemiluminescence, both at the middle of the light period and at the

447 end of the dark period (Fig. 9B). In good agreement with the EPR results, the luminescence

448 signal was significantly lower in LD than in SD in WT illuminated leaves, while it was not

449 markedly different in the mutant. Therefore, although ROS content of illuminated leaves was

450 lower in *ndufs8.1 ndufs8.2* than in the WT under SD, they were similar in both genotypes

451 under LD. As observed in the light, ROS contents of both genotypes were lower in LD than in

452 SD at the end of the dark period. However, in contrast to the middle of the light period, dark

453 ROS content tended to be higher in the mutant than in the WT, maybe reflecting altered

454 mitochondrial metabolism.

455   We further examined transcript levels of oxidative stress markers in different cell

456 compartments: mitochondrial alternative oxidase *AOX1a* (Saisho et al., 1997) and external

457 NAD(P)H dehydrogenase *NDB2* (Michalecka et al., 2003; Yoshida and Noguchi, 2009),

458 chloroplastic ferritin *FER1* (op den Camp et al., 2003), cytosolic ascorbate peroxidase *APX1*

459 (Koussevitzky et al., 2008) and peroxisomal catalase *CAT2* (Noctor et al., 2007). In

460 illuminated SD leaves, expression levels of antioxidant enzymes were not higher in the

461 *ndufs8.1 ndufs8.2* mutant than in the WT, and they were increased under LD in both

462 genotypes, except for *CAT2* mRNAs that were increased only in the WT (Fig. 9C). Although

463 *NDB2* transcripts accumulated proportionally more in the mutant than in WT, *AOX1a* were

464 similar in both genotypes, regardless of the photoperiod. This was unexpected since the AOX

465 protein was found to be more abundant in the mutant under greenhouse conditions (Fig. 3C).

466 In order to examine whether *AOX1a* transcript accumulation might respond to light intensity,

467 SD and LD plants were transferred to 200 µmol m^{-2} s^{-1} PAR for 3 days. Under these

468 conditions, *AOX1a* transcripts appeared to be markedly higher in the mutant than in the WT

469 in LD, whilst *CAT2* levels were less abundant (Supplemental Fig. S16A), showing a crossed

470 effect of illumination and photoperiod. When plants were grown in the greenhouse in LD,

471 *AOX1a* and *NDB2* mRNAs were also more abundant in the mutant than in the WT at middle

472 of the light period, in contrast to other redox markers (Supplemental Fig. S16B). In addition,

473 transcript levels of *AOX1a*, *NDB2, APX1* and *BAP1* (Bonzoi associated protein 1, a marker of

474 oxidative stress in the chloroplastic compartment, op den Camp et al., 2003), were

475 considerably lower at the end of the dark period than at middle of the light period in both

476 genotypes (Supplemental Fig. S16B).

477   Previous work has shown that redox homeostasis of CMSII plants in LD condition

478 was associated to activation of the enzymatic antioxidant system (Dutilleul et al., 2003b).

479 Similarly, we found higher detoxification activities in *ndufs8.1 ndufs8.2-* than in WT plants

480 under both photoperiods (Supplemental Fig. S17). Both catalase (CAT, the major H$_2$O$_2$-

481 detoxifying enzyme in plant leaves, Willekens et al., 1997) and non-chloroplastic ascorbate

482 peroxidase (*i.e.* cytoplasmic cAPX) activities were significantly higher in the mutant under

483 SD, whereas glutathione reductase (GR) (a key enzyme of the ascorbate-glutathione cycle,

484 Foyer and Noctor, 2011) was higher under LD. In both genotypes, antioxidant activities were

485 hardly affected by photoperiod, except cAPX that was clearly inhibited under LD. In addition,

486 the mutant had higher levels of anthocyanins (involved in redox control in Arabidopsis,

487 Vanderauwera et al., 2005) than in the WT under both photoperiods, especially during the

488 first 3 days following transfer from SD to LD (Supplemental Fig. S17). Hence, our results

489 indicate that the *ndufs8.1 ndufs8.2* mutant does not exhibit a general oxidative stress in either

490 SD or LD, likely because of the induction of antioxidant activities. However, the photoperiod

491 and light/dark responses appeared to be altered, possibly reflecting some differences in

492 subcellular distribution of ROS, in particular mtROS accumulation.

493

494 ***Photoperiod differentially modulates soluble antioxidants and* redox co-factors *in WT,***

495 **ndufs8.1 ndufs8.2 *and* ndufs4 *plants***

496

497 In addition to high activity of antioxidant enzymes in CMSII (Dutilleul et al., 2003b;

498 Vidal et al., 2007), CI mutants contain more soluble redox buffers than the WT in LD

499 condition (Dutilleul et al., 2005; Kühn et al., 2015). Here, we found that total leaf glutathione

500 (GSH and GSSG for reduced and oxidized forms, respectively) and ascorbate (both reduced

501 and oxidized form, dehydroascorbate) were higher in both *ndufs8.1 ndufs8.2* and *ndufs4*

502 mutants than in the WT under both SD and LD, accompanied by slightly higher oxidation

503 (Fig. 10A). Noticeably, levels of both redox buffers were higher in *ndufs4* than in *ndufs8.1*

504 *ndufs8.2* in SD. Transfer to LD resulted in a 30% glutathione increase in WT and *ndufs8.1*

505 *ndufs8.2*, whereas levels were unchanged in *ndufs4*. No significant differences in ascorbate

506 content between SD and LD conditions were observed independently of genotype.

23

507   In contrast to redox buffers, NAD(H) content was higher in *ndufs8.1 ndufs8.2* than

508   in WT under SD condition only, whereas *ndufs4* displayed higher contents under both

509   photoperiods (Fig. 10B). A clear build-up in total leaf NAD(H) was observed under LD in the

510   WT but not in the mutants. Under both photoperiods, the NAD pool was more reduced (larger
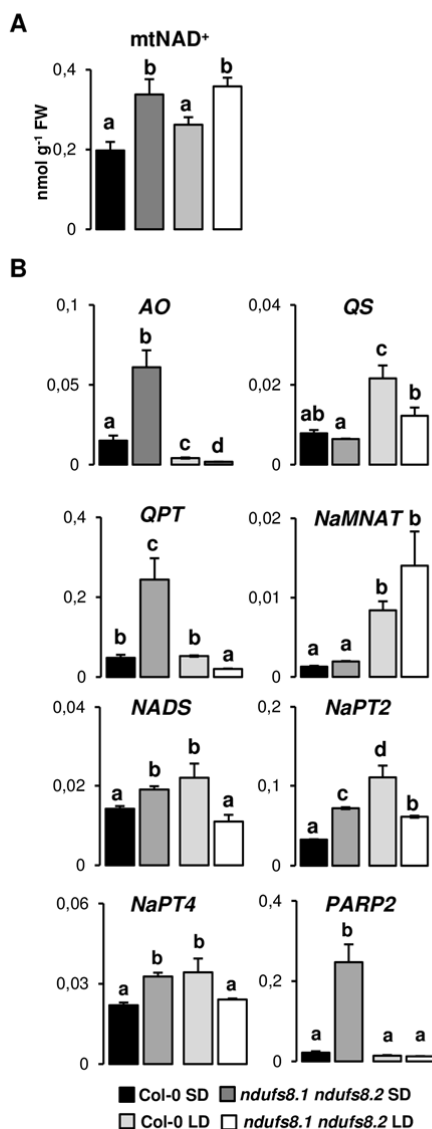
Figure 11. Pools of mitochondrial NAD⁺ and transcriptional analysis of NAD⁺ biosynthetic genes

In all experiments, leaves were sampled from SD12/LD12 Col-0 and *ndufs8.1 ndufs8.2* plants at the middle of the day period. **A**, NAD⁺ contents (nmol g⁻¹ FW) of mitochondrial preparations. Results are means +SE of at least 3 extracts from different plants. Different letters indicate significant differences according to Student *t* test.
B, RT-qPCR analyses of NAD⁺ biosynthetic genes were carried out using *ACT2* as a reference. Aspartate oxidase (*AO*), quinolinate synthase (*QS*), quinolinate phosphoribosyltransferase (*QPT*), nicotinate mononucleotide adenylyltransferase (*NaMNAT*), NAD synthetase (*NADS*) and nicotinate hosphoribosyltranferase 2,4 (*NaPT2, 4*) and Poly-ADP-ribose polymerase 2 *(PARP2)*. Results are means + SE of at least 6 extracts from different plants. Different letters indicate significant differences according to Student *t* test.

511   NADH/ NAD⁺ ratio) in the mutants than in Col-0. Interestingly, mtNAD⁺ levels determined

512   in Percoll-purified leaf mitochondria were not significantly affected by the photoperiod, and

513   were higher in the mutant than in the WT under both SD and LD (Fig. 11A). Total leaf
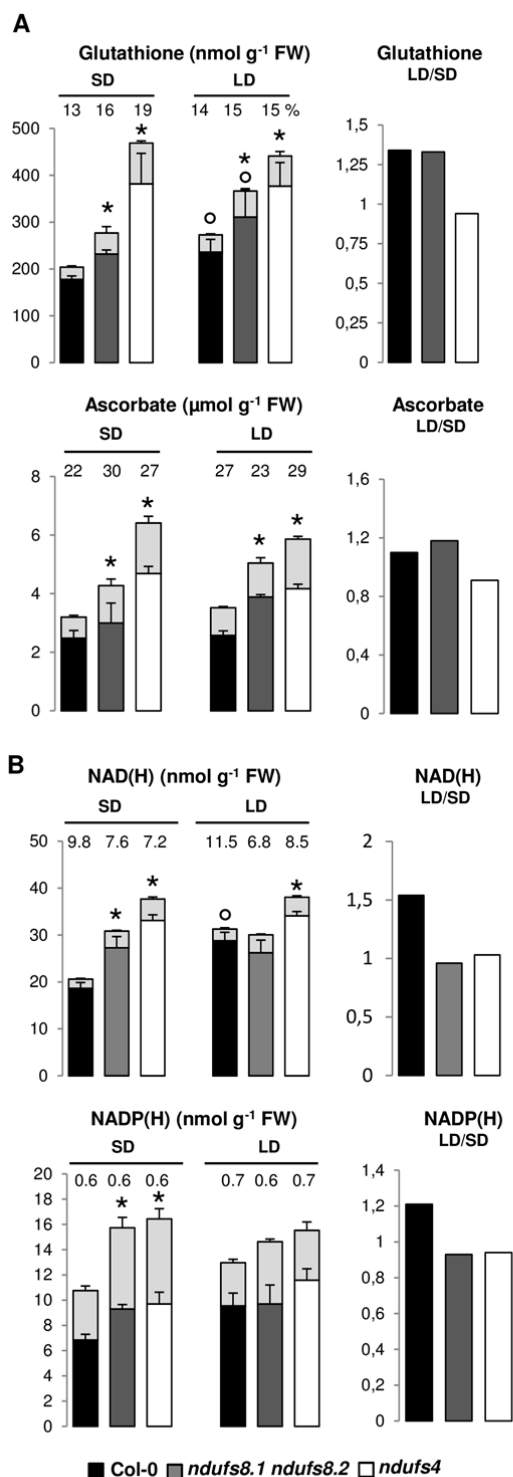
Figure 10. Pools of foliar redox buffers and co-factors of Col-0, *ndufs8.1 ndufs8.2* and *ndufs4* plants
Leaves were sampled from SD6/LD6 plants at the middle of the day period. Black columns: Col-0; dark grey columns: *ndufs8.1 ndufs8.2*; white columns: *ndufs4*

A, Redox buffers
 - Left: total leaf content of reduced and oxidized (top, light grey) forms of glutathione (nmol g⁻¹ FW) and ascorbate (µmol g⁻¹ FW). Redox state (% of oxidised forms) are indicated on top of the histograms. Data are means +SE from at least 4 extracts from different plants;
* indicate significant differences (P<0.05) between WT and mutant total pools according to Student t test; ° indicate significant differences between SD and LD values for the same genotype.
- Right: LD/SD ratios in the three genotypes.

B, Redox co-factors
 - Left Total leaf content of oxidized and reduced (top, light grey) forms of NAD(H) and NAD(P)H (nmol g⁻¹ FW); NAD(P)⁺/NAD(P)H ratios are indicated on top of the histograms. Results are means +SE of at least 8 extracts from different plants; * indicates significant differences (P<0.05) between WT and mutant total pools according to Student t test; ° indicates significant differences between SD and LD values for the same genotype.
- Right: LD/SD ratios in the three genotypes.

514   NADP(H) contents were also higher in the mutants than in the WT under SD, and a slight
515   photoperiod effect was observed in the WT only (Fig. 10B).
516   In order to determine whether NAD⁺ contents might be regulated at the
517   transcriptional level, we performed RT-qPCR analyses of genes involved in either *de novo*

26

518   NAD$^+$ biosynthesis or NAD$^+$ recycling (Noctor et al., 2006): aspartate oxidase *(AO,* the first

519   enzyme of the *de novo* pathway in plants, Katoh et al., 2006), quinolinate synthase (*QS*),

520   quinolinate phosphoribosyltransferase (*QPT),* nicotinate mononucleotide adenylyltransferase

521   (*NaMNAT*), NAD synthetase (*NADS*) and nicotinate phosphoribosyltranferases (*NaPT2/4*).

522   We also examined expression of *PARP2* (Poly-ADP-ribose polymerase 2) that uses NAD$^+$ as

523   a substrate in stress responses (Schreiber et al., 2006). There were considerable differences in

524   gene expression between genotypes and photoperiods (Fig. 11B). Under SD, the high leaf

525   NAD$^+$ content of the mutant (as compared to WT) was accompanied by an accumulation of

526   *AO*, *QPT, NADS, NaPT2/4* and *PARP2* transcript*s*. In Col-0, *NADS, QS, NaMNAT* and

527   *NaPT2/4* transcripts were more abundant in LD than in SD, thereby matching the higher

528   NAD$^+$ content. In contrast, *AO, NADS, QPT, NaPT2/4* and *PARP2* transcript levels were

529   lower in the mutant in LD than in SD condition.

530   Hence, the loss of CI activity in both mutants is associated with *(i)* accumulation of

531   redox cofactors under SD conditions, and *(ii)* impaired redox acclimation to LD condition.

532

533

27

534   **Discussion**

535

536   ***Lack of the NDUFS8 subunit results in holo-CI mis-assembly and remodeling of the***
537   ***respiratory chain***

538

539   The NDUFS8 CI subunit is highly conserved from bacteria to Eukaryotes including
540   plants (Klodmann et al., 2010). It is located in the Q module and binds two 2S-4Fe clusters
541   involved in electron transfer to ubiquinone (Efremov et al., 2010). NDUFS8 was found to be
542   required for holo-enzyme assembly and activity in bacteria and humans (Procaccio and
543   Wallace, 2004). In contrast to other species investigated (except *Brassica rapa*), Arabidopsis
544   NDUFS8 is encoded by two genes, *NDUFS8.1* and *NDUFS8.2* (Fig. 1A) expressed in
545   different tissues (Schmid et al., 2005; Qin et al., 2009), but their respective role has not been
546   established so far. We found that *NDUFS8.2* is about 2.5 times more expressed than
547   *NDUFS8.1* in Col-0 seedlings and rosette leaves (Fig. 1C). Despite the lack of visible
548   compensation at the transcript level, neither single mutants showed any apparent differences
549   in CI assembly/activity (Fig. 2), indicating that post-transcriptional/ translational controls
550   occurred or, alternatively, that NDUFS8 amount was not limiting. These results indicate that
551   the two NDUFS8 subunits have similar roles in CI assembly, forming complexes able to
552   display normal NADH dehydrogenase activity. Interestingly, although no phenotypic
553   alterations were observed in single mutants grown under greenhouse conditions, *in vitro*
554   germinating seedlings display a slightly reduced growth rate, suggesting that presence of both
555   subunits is beneficial at some development stages, in particular before autotrophy. Further
556   investigations are required to establish potential differences in the composition of the CI
557   complex in different tissues and environments.

558   In contrast to the single mutants, the *ndufs8.1 ndufs8.2* double mutant has
559   undetectable levels of both transcripts (Fig. 1C) and lacks detectable holo-CI
560   assembly/activity. This clearly evidences the absence (or only residual amounts) of the
561   NDUFS8 subunit in the double mutant and its central role in holo-CI assembly in plants.
562   Although traces of holo-CI could not be detected using immunochemistry using anti NAD9-
563   and anti-CA2 antisera or NDH/NBT in-gel assays in *ndufs8.1 ndufs8.2*, very low levels of
564   polypeptides potentially corresponding to CI subunits can be distinguished using 2D BN/
565   SDS-PAGE (Supplemental Fig. S1), suggesting that sub-stoichiometric amounts of the
566   complex might indeed be present. Furthermore, sub-complexes might be assembled, as

567   reported for many CI mutants lacking either peripheral or membrane subunits in plants

568   (Karpova and Newton, 1999; Brangeon et al., 2000; Pineau et al., 2008; Meyer et al., 2009;

569   Kühn et al., 2015; Soto et al., 2015) and humans (Vogel et al., 2007). A specific mt CA signal

570   was as abundant in *ndufs8.1 ndufs8* than in Col-0 mt proteins (Fig. 3C), suggesting that sub-

571   complexes associated to the CA domain (possibly assembly intermediates, see Wang et al.,

572   2012) might be present in this mutant as previously reported in *ndufs4* (Kühn et al., 2015).

573   Besides potential traces of holo-CI, the induction of alternative respiratory enzymes

574   might be crucial to sustain respiration in *ndufs8.1 ndufs8.2*. In addition to Complex II

575   (succinate dehydrogenase), non-phosphorylating alternative NAD(P)H dehydrogenases (type

576   II dehydrogenases), located on the inner and outer surface of the inner mitochondrial

577   membrane, are essential for plant growth and metabolism (Liu et al., 2009; Wallström et al.,

578   2014). Their activity depends on plant metabolic status, such as NADH and Ca^{2+}

579   concentration (Rasmusson et al., 2008). The stimulation of both internal and external enzymes

580   was reported in the tobacco CMSII and NMS1 mutants (Sabar et al., 2000), and induction of

581   external enzymes was reported in maize NCS2 (Marienfeld and Newton, 1994) and in *ndufs4*

582   (Meyer et al., 2009). Similar to CMSII and *ndufs4* mutants (Meyer et al., 2009; Kühn et al.,

583   2015), total respiration measured either as oxygen consumption (Fig. 3A) or as CO_2 emission

584   (Fig. 8A), was not altered in *ndufs8.1 ndufs8.2* LD leaves, indicating that the electron flux

585   through alternative NAD(P)H dehydrogenase(s) was stimulated in the mutant. Consistently,

586   we found an accumulation in mitochondrial NAD(H) in *ndufs8.1 ndufs8.2* (Fig. 11A), as

587   would be expected considering the low affinity for NADH of these enzymes (Møller, 2001).

588   Also, as reported for other CI mutants including *ndufs4* (Sabar et al., 2000; Karpova et al.,

589   2002; Meyer et al., 2009; Keren et al., 2012; Cohen et al., 2014), increased AOX protein

590   content and capacity were observed in *ndufs8.1 ndufs8.2* (Fig. 3B and Fig. 3C). Interestingly,

591   AOX accumulation was accompanied by reduced aconitase transcript levels (Supplemental

592   Fig. S13) and increased content in citrate (Fig. 6, Fig. 7 and Fig. S9), a well-known AOX

593   activator (Vanlerberghe and McIntosh, 1996). High electron partitioning to AOX could have

594   allowed re-oxidation of excess of NADH in the mitochondrial matrix caused by CI

595   impairment, while the COX pathway is essentially controlled by ATP (Florez-Sarasa et al.,

596   2007). Here, since alternative pathways are non-phosphorylating (not coupled to H^+

597   translocation), the ATP yield of mitochondrial electron transport is expected to be reduced in

598   *ndufs8.1 ndufs8.2,* as reported in CMSII (Sabar et al., 2000) and *ndufs4* (Meyer et al., 2009).

599   In summary, there is an induction of alternative respiratory pathways in *ndufs8.1 ndufs8.2*

600   similar to most CI mutants investigated so far. However, in contrast to CMSII (Vidal et al.,

601   2007; Priault et al., 2007), the *in vivo* electron partition to AOX is increased in *ndufs8.1*
602   *ndufs8.2*.

603

604   ***Large reduction of CI activity results in a similar phenotype in ndufs8.1 ndufs8.2 and***
605   ***ndufs4 mutants grown under LD condition.***

606

607   Plant CI mutants have different phenotypes, from mild (growth retardation only, as in
608   *ndufs4*), to severe (morphological defects as in tobacco CMSII, NMS1 and maize *ncs2*), or
609   even near-lethal (*nMat, ndufv1*) (see Introduction). Here, we found that the *ndufs8.1 ndufs8.2*
610   double mutant displays a mild phenotype, without phenotypic alterations at the adult stage in
611   flowering conditions (LD) (Supplemental Fig. S3). The slow-growing phenotype is clearly
612   related to holo-CI highly reduced contents in the double mutant, as both single mutants had
613   CI assembly/activity and growth rates identical to the WT. This also indicates the absence of
614   unidentified insertions in the mutants, at least insertions with phenotypic consequences.
615   Despite very slight differences in germination (+ 30%) and seedling growth rates (+20%),
616   *ndufs8.1 ndufs8.2* plants were similar to *ndufs4* plants at subsequent developmental stages
617   (Supplemental Fig. S3 and Fig. S4). The mild phenotype of the *ndufs4* mutant has been
618   suggested to result from persisting trace amounts of CI activity (Kühn et al., 2015). Although
619   we were unable to detect an NDH/NBT signal around 1 MDa in *ndufs8.1 ndufs8.2* BN PAGE
620   (Fig. 2), low levels of CI activity cannot be excluded, since sub-stoichiometric amounts of
621   putative CI subunits are detected by 2D BN/SDS PAGE (Supplemental Fig. S1).
622   Nevertheless, it is not possible to estimate accurately possible differences in sub-
623   stoichiometric holo-CI levels between *ndufs8.1 ndufs8.*2 and *ndufs4* mutants due to the
624   limited sensitivity of detection methods (discussed in Keren et al., 2012).

625   As for other CI mutants, the lower efficiency of the respiratory chain (discussed
626   above) might explain the slow-growth phenotype of *ndufs8.1 ndufs8.2* LD plants. Similar to
627   *nMat, ndufs4* and *ndufv1* mutants (Keren et al., 2012; Kühn et al., 2015), sucrose
628   supplementation improves *in vitro* development of *ndufs8.1 ndufs8.2* seedlings (Supplemental
629   Fig. S3D), suggesting that photosynthetic ATP might compensate for lower mtATP
630   production. Nevertheless, as previously reported for CMSII (Szal et al., 2008; Djebbar et al.,
631   2012) and *ndufs4* (Meyer et al., 2009), total leaf ATP of illuminated leaves was not affected
632   in *ndufs8.1 ndufs8.2* (Fig. 3B), indicating either activation of alternative mechanisms of ATP
633   production as substrate-level phosphorylation at the level of mitochondrial enzymes, as
634   proposed by Kühn et al. (2015), or reduced rates of cellular processes resulting in a lower

30

635   ATP consumption. Regardless of the exact specific mechanism(s) involved, the growth

636   retardation phenotype of CI mutants in LD condition is unlikely to be related to energy

637   limitation.

638   Oxidative stress might also be involved in the reduced growth of CI mutants.

639   Accordingly, ROS accumulation has been reported to occur in several Arabidopsis CI

640   mutants, including *ndufs4* (Meyer et al., 2009), in possible relation to increased mtROS

641   generation by the remodeled respiratory chain. High levels of AOX proteins and capacities in

642   all CI mutants investigated so far are in line with this hypothesis. However, alike CMSII and

643   NMS1 mutants (Dutilleul et al., 2003b), ROS accumulation could not be observed in

644   illuminated leaves of *ndufs8.1 ndufs8.2* using various methods (Fig. 9 and Supplemental Fig.

645   S15), likely due to the over-activation of antioxidant enzymes (Supplemental Fig. S17).

646   Therefore, a marked oxidative stress is unlikely to have impeded growth rates under LD in

647   this mutant, although such an effect cannot be excluded in *ndufs4*.

648   Metabolic perturbations associated with respiration re-orchestration might account

649   for the slow growth phenotypes of *ndufs8.1 ndufs8*.2 and *ndufs4* mutants. In fact,

650   mitochondria are known to play a key role in the nitrogen/carbon balance (Foyer et al., 2011),

651   which is affected in CMSII, with a marked increase in amino acids plausibly caused by high

652   NAD(H) content (Dutilleul et al., 2005; Hager et al., 2010; Djebbar et al., 2012). Similarly,

653   we found here that despite lower values for parameters associated with nitrate assimilation

654   (that is, *NR* transcripts, NR activity and NO_3^- content), amino acids accumulated in both

655   mutants, with the notable exception of aspartate (which appeared to be decreased except at the

656   end of the night, Fig. 6 and Supplemental Fig. S9). However, we did not observe a significant

657   NAD(H) build-up in *ndufs8.1 ndufs8.2* leaves as compared to the WT in LD (Fig. 10B),

658   suggesting that an increase in NAD(H) content per se is not the cause of amino acid

659   accumulation in the mutants. Rather, amino acid accumulation clearly paralleled that of

660   carbon skeletons generated by TCA cycle-activity (citrate, succinate, fumarate and malate) in

661   both mutants. It thus suggests that in the light, when a partial TCA cycle is believed to operate

662   (Tcherkez et al., 2009; Sweetlove et al., 2010), the metabolism in mutants is associated with:

663   *(i)* a stimulation of both cytosolic and mitochondrial malate dehydrogenases (whereby

664   oxaloacetate is rapidly reduced to malate) because of over-reduced NAD(H) (Heldt et al.,

665   2004; Tomaz et al., 2010); and *(ii)* an increased PEPc activity (OʼLeary et al., 2011) as

666   reported in CMSII mutants (Dutilleul et al., 2005), at the expense of aspartate accumulation.

667   In the night, the operation of the 'full' (cyclic) TCA cycle and thus the lower reduction of

668   oxaloacetate to malate would account for the high aspartate observed in *ndufs8.1 ndufs8.2*

669   mutant.

670   Hence, our results show a similar impact of reduced CI activity in both *ndufs8.1*

671   *ndufs8.2* and *ndufs4* mutants at developmental, physiological and metabolic levels, in relation

672   with NAD(H) over-reduction.

673

674   **The growth-retardation phenotype is more pronounced in ndufs4 *than in* ndufs8.1**

675   **ndufs8.2 *plants grown in SD condition in possible relation to higher oxidative stress***

676

677   All plant CI mutants characterized so far display growth retardation in LD, associated to

678   various physiological and metabolic alterations but their phenotype in SD has never been

679   documented. Here, we show that *ndufs8.1 ndufs8.2* and *ndufs4 plants* had a retarded growth

680   phenotype under both LD and SD conditions (Fig. S4). However, in contrast to LD, the

681   retardation phenotype was more marked in *ndufs4* than in *ndufs8.1 ndufs8.2* plants under SD,

682   sometimes associated with necrotic spots. Although accumulation of total soluble redox

683   buffers, glutathione and ascorbate, was observed in mutants under both SD and LD, redox

684   buffers were in significantly higher amounts in *ndufs4* as compared to *ndufs8.1 ndufs8.2*

685   under SD (Fig. 10A), strongly suggesting enhanced oxidative stress. This effect might have

686   originated from a less activated mitochondrial antioxidant system in *ndufs4* compared to

687   *ndufs8.1 ndufs8.2*. In fact, in contrast to *ndufs4* (Meyer et al., 2009), *NDB2* and *AOX1a*

688   transcripts accumulated in *ndufs8.1 ndufs8.2* either under our standard illumination condition

689   (100 µmol photons m^{-2} s^{-1}, Fig. 9C) or at high light (Supplemental Fig. S16). Redox

690   differences between *ndufs4* and *ndufs8.1 ndufs8.2* might result from the nature and/or location

691   of the lacking CI subunit. In *ndufs4*, large accumulation of the CA domain, which was

692   proposed to be involved in plant CO_2 transport (Zabaleta et al., 2012) and carbon metabolism

693   (Soto et al., 2015; Fromm et al., 2016), might result in increased mtROS production, as

694   reported in animals (Price et al., 2011). NDUFS4 and NDUFS7 are located in different CI

695   modules (N and Q respectively) and in human cell lines, mitochondrial metabolism was

696   differentially affected in mutants affected in the two modules, in relation to differential

697   accumulation of assembly intermediates (Leman et al., 2015).

698   Untargeted metabolomics showed that the reduced growth of *ndufs4* as compared to

699   *ndufs8.1 ndufs8.2* SD plants was accompanied by much larger differences in global

700   metabolism under SD than under LD (Fig. 5), in particular by higher levels of many amino

701   acids (Fig. 6), as previously reported for low N adapted plants (Tschoep et al., 2009). It is

702   interesting to note that the metabolomics signature of *ndufs4* SD leaves has some similarities

703   to that of plants under anoxic stress (Sousa and Sodek, 2002; Sweetlove et al., 2010).

704   Similarity to the anoxic response can also be found in citrate accumulation, low level of

705   aconitase transcripts and increased AOX capacity in *ndufs8.1 ndufs8.2* (Fig. 3, Fig. 6 and

706   Supplemental Fig. S13), as shown by Gupta et al. (2012). Also, the CMSII mutant displays

707   up-regulation of fermentation pathways (Shah et al., 2013).

708   Overall results indicate that redox state is more compromised in *ndufs4* in SD than in

709   LD condition, possibly resulting in the redirection of TCA fluxes towards amino acid

710   synthesis at the expense of oxidative phosphorylation, therefore explaining the lower growth

711   rates.

712

713   ***Growth and metabolic acclimation to LD depend on CI activity***

714

715   The rapid growth acceleration observed in Col-0 plants after their transfer to LD

716   (already visible at day 3, Fig. 4) was clearly reduced in the *ndufs8.1 ndufs8.2* mutant.

717   Moreover, physiological changes associated with the SD-to-LD transition in the WT (such as

718   an increased leaf mass area (LMA), palisade cell width, stomatal conductance, carboxylation

719   efficiency, dark respiration, total ATP, and decrease in nitrogen assimilation and total ROS

720   levels) were not observed (or highly reduced) in the mutant (Fig. 8 and Supplemental Fig.

721   S5), thereby showing an impaired acclimation to LD. Despite marked growth differences

722   between *ndufs8.1 ndufs8.2* and *ndufs4* under SD conditions, the growth response of both

723   mutants, taken at a similar developmental stage (9-leaf stage), to the SD-to-LD transition was

724   comparably impaired as compared to WT (Fig. 4). Untargeted metabolomics (HILIC-qTOF-

725   MS) and GC-TOF analyses confirmed that metabolism was less affected in both mutants than

726   in WT upon SD-to-LD transfer (Fig. 5). The differential photoperiod effect on TCA

727   intermediates, amino acids and redox buffers in mutants (Fig. 6 and Fig. 10A) likely reflected

728   their different metabolic and redox states under SD (as discussed before). That is, it is

729   unlikely that the altered content in respiratory metabolites was the cause for the impaired

730   photoperiod acclimation.

731   Rather, we found a clear correlation between the lack of NAD(H) accumulation and

732   impaired LD acclimation in both *ndufs8.1 ndufs8.2* and *ndufs4* mutants. In fact, in contrast to

733   WT, NAD(H) contents *(i)* were high under SD condition, as would be anticipated considering

734   high K_m(NADH) values of alternative NADH dehydrogenases and *(ii)* did not significantly

735   increase in both mutants under LD (Fig. 10B). Presumably, NAD^+ accumulation in WT plants

736   transferred to LD came from a complex set of interactions between biosynthesis, oxidation by

737 the mtETC (higher dark respiration) and degradation. A reduced NAD^+ consumption under

738 LD is suggested by the decreased levels of *PARP2* transcripts (Fig. 11B). Also, in *ndufs8.1*

739 *ndufs8.2*, there was higher expression of several transcripts encoding NAD^+ biosynthesis

740 enzymes under SD and a clear depressing effect of LD, suggesting repression of NAD^+

741 neosynthetic/recycling pathways under LD.

742   Overall, our data show that the physiological and metabolic re-orchestration

743 accompanying LD acclimation in Arabidopsis is similarly compromised in both *ndufs8.1*

744 *ndufs8.2* and *ndufs4* mutants, thereby strongly suggesting that it results from reduced CI

745 activity.

746

747 **Signaling mechanisms possibly involved in impaired LD acclimation of CI mutants**

748

749   Changes in the composition of mitochondrial enzymes in CI mutants are expected to

750 generate increased ROS by the mtETC. In fact, ROS were previously reported to accumulate

751 in several plant CI mutants (Meyer et al. 2009; Keren et al., 2012) and in human cell lines

752 lacking CI peripheral arm subunits (Verkaart et al., 2007; Miwa et al., 2014), where they were

753 produced by matrix intermediates (Leman et al., 2015). Although total ROS levels were

754 similar in *ndufs8.1 ndufs8.2* and WT in the middle of the light period, they were higher in the

755 mutant than in the WT at the end of night period (Fig. 9B), thus suggesting increased

756 generation of mtROS by the respiratory chain. A general role of mtROS in plant signaling is

757 well documented (Huang et al., 2016). In humans, mtROS were reported to induce PDH

758 (pyruvate dehydrogenase) activity by inactivating PDHK2 (pyruvate dehydrogenase kinase 2)

759 (Hurd et al., 2012)*,* thereby supporting a pathway through which mtROS may regulate

760 respiratory metabolism. Therefore a specific signaling role for mtROS in the photoperiod

761 response is possible.

762   Also, glutathione levels and redox state have been reported to regulate day length

763 transcriptional responses in the *cat2* mutants (Queval et al., 2007a). Here, we found that

764 although antioxidants were higher in both mutants, they were differentially affected by

765 photoperiod: glutathione and ascorbate accumulated under LD in WT and in *ndufs8.1*

766 *ndufs8.2,* but not in *ndufs4* maybe because of the high content in SD (Fig. 10A). Therefore,

767 antioxidants per se are unlikely to be involved in the impairment of the photoperiod response

768 in CI mutants. In contrast, NAD(H) increased in LD in WT but not in both mutants, thereby

769 correlating to growth rates in the three genotypes (see above). NAD^+ is known to be involved

770 in the control of Arabidopsis growth (Hashida et al., 2009). In addition to its well-established

771   role in redox homeostasis and oxidative phosphorylation, a considerable body of evidence

772   indicates that NAD^+ is a crucial signaling molecule (Sassone-Corsi, 2012; Pétriacq et al.,

773   2012, 2013, 2016) driving mitochondrial oxidative metabolism in mammals (Mouchiroud et

774   al., 2013; Rey and Reddy, 2013). In animals, the inhibition of nicotinamide phosphoribosyl

775   transferase (NAMPT), involved in nicotinamide recycling into NAD^+, has been found to

776   impede glycolysis and TCA cycle activity, and lead to ATP depletion (Tan et al., 2013).

777   A slight but consistent over-reduction of NAD(H) was observed in both Arabidopsis

778   mutants (NAD^+/NADH around 7-8 % under all conditions, compared to 10-11% in the WT

779   (Fig. 12B), as previously found in CMSII (Hager et al., 2010). Reduction levels of pyridine

780   nucleotides are believed to exert a control on TCA fluxes (Igamberdiev and Gardeström,

781   2003; Araújo et al., 2012), for example by controlling mtMDH activity (Tomaz et al., 2010).

782   This effect could explain the lack of significant respiratory increase in *ndufs8.1 ndufs8.2*

783   under LD (Fig. 8A). Over-reduction of the NAD pool in mutants might stem from the

784   induction of alternative NAD(P)H dehydrogenase activities (Liu et al., 2009; Rasmusson and

785   Wallström, 2010; Wallström et al., 2014) and/or activation of redox shuttles (Shen et al.,

786   2006). A redox effect may have then resulted in alterations of the circadian clock (Stangherlin

787   and Reddy, 2013; Shim and Imaizumi, 2015). Indeed, NAD^+ is a clock-regulated metabolite

788   in animals (Peek et al., 2013) and alteration of clock regulator expression during LD

789   acclimation (Fig. 8D) and the dramatic increase in anthocyanins (Supplemental Fig. S17),

790   which are regulated by cryptochromes (Ahmad et al., 1995), might reflect perturbation of the

791   circadian clock in the *ndufs8.1 ndufs8.2* mutant. This would be similar to what was reported

792   in mutants affected in promoter regions of genes encoding mitochondrial proteins (Giraud et

793   al., 2010). Interestingly, diurnal rhythms of *AOX* expression are highly perturbed in the

794   CMSII mutant, possibly reflecting an impaired circadian cycle (Dutilleul et al., 2003b).

795   Conversely, it has been shown that Arabidopsis mutants affected in circadian clock regulation

796   exhibit dramatic changes in mitochondrial metabolome, in particular TCA derivatives

797   (Fukushima et al., 2009). Thus, we hypothesize that an impairment in the circadian clock

798   occurred in the CI mutants examined here, thus leading to metabolic perturbations (Peek et

799   al., 2012; Haydon et al., 2015) and limited growth enhancement under LD conditions. The

800   specific signaling mechanisms linking CI to circadian clock regulation nevertheless need

801   further investigation.

802

803   **Conclusion**

804   In summary, our study provides compelling evidence that photoperiod influences the

805   phenotype of Arabidopsis CI mutants. Despite lower growth of *ndufs4* in SD (possibly related

806   to a higher oxidative stress), *ndufs8.1 ndufs8.2* and *ndufs4* showed an impaired acclimation to

807   LD after growth in SD, associated with a differential re-orchestration of metabolism. We

808   propose that highly reduced CI activity, *i.e.* oxidation of mitochondrial NADH, affects

809   photoperiod acclimation *via* mtROS and/or NAD(H) content and redox state.

810
811
812

813   **Material and Methods**

814

815   **Plant Material**

816   Arabidopsis seeds of the SAIL_227F03 line carrying a T-DNA insertion in the *At1g16700*

817   gene (further referred to as *NDUFS8.1*), and of the SALK_062179 line carrying an insertion

818   in the *At1g79010* gene (further referred to as *NDUFS8.2*), were selected using the T-DNA

819   express Arabidopsis gene mapping tool (http://signal.salk.edu/cgi-bin/tdnaexpress, Alonso et

820   al., 2003) and ordered from the Nottingham Arabidopsis Stock Centre. Both mutant lines

821   come from T-DNA mutagenized population in the Col-0 Arabidopsis ecotype. Primers used

822   are listed in Supplemental Table 1 online. For initial characterization of single and double

823   mutants, plants were grown in greenhouses under a 16h photoperiod, at a day/night

824   temperature regime of 23°C/17°C, under natural illumination supplemented with artificial

825   lighting as described in Vidal et al. (2007). In addition, seeds of the *ndufs4* mutant were

826   kindly provided by E. Meyer. For LD/SD comparisons, WT and *ndufs8.1 ndufs8.2 /ndufs4*

827   seeds were sown at one week of interval and seedlings were grown in controlled chambers in

828   SD (8h/16h, day/night) at 100 µmol m^{-2} s^{-1} PAR up to reach the 8-9 leaf stage (stage referred

829   to as SD0 thereafter). After this time point, rosette plantlets were either transferred to LD

830   (16h/8h) or maintained under SD conditions under the same illumination conditions. Licor®

831   measurements were performed on well-developed leaves of 2-3 month old rosette plants

832   (minimum 2 cm^2 area). In all cases, experiments were carried out on mutant and Col-0 plants

833   of similar development.

834

835   **RNA isolation and RT-PCR analysis**

836   Total RNA was prepared using the Trizol reagent (Invitrogen, Carlsbad, CA, USA), following

837   the manufacturer's recommendation. RNA (1 µg) was treated with RQ1 RNase-Free DNase

838   (Promega, Madison, WI, USA) and reverse-transcribed using random hexamers and

839   SUPERSCRIPT™ III First-strand kit (Invitrogen, Carlsbad, CA, USA) following the

36

840   manufacturer's recommendations. LightCycler® 480 detection system (Roche Applied

841   Science) was used to perform quantitative real-time PCR. Relative mRNA abundance was

842   calculated using the comparative delta-Ct method and normalized to the corresponding

843   *ACTIN2* (*At3g18780*) gene levels. The sequences of primers used in this study are listed in

844   Supplemental Table 1.

845

846   **CO$_2$ exchange measurements**

847   Responses of net carbon assimilation (A) to PFD (light curves) and internal CO$_2$ molar

848   fraction (A/Ci curves) performed under ambient (21%) oxygen content were measured on

849   attached leaves with an open infrared gas analysis system equipped with a leaf chamber

850   fluorometer (Li-Cor 6400-40; Li-Cor Inc., Lincoln, NE, USA), as described in Priault et al.

851   (2006a). Leaves were dark adapted for at least 30 min before determining dark respiration.

852

853   **Oxygen respiratory measurements**

854   Oxygen isotope discrimination experiments were performed as in Florez-Sarasa et al. (2007),

855   under controlled conditions (12 h/12 h photoperiod), except that plants were grown under 80

856   μmol.m^{-2}.s^{-1}; oxygen-isotope fractionation calculations were made as described Guy et al.

857   (1989) and Ribas-Carbo et al. (1995). The alternative oxidase (AOX) pathway capacity was

858   measured on leaf tissues as in Florez-Sarasa et al. (2009).

859

860   **Preparation of crude leaf and root membrane extracts, Blue Native electrophoresis,**

861   **Western analyses and determination of in-gel NADH dehydrogenase activity**

862   Extraction of total and mitochondrial proteins, BN-PAGE, two-dimensional BN/SDS

863   electrophoresis, determination of *in gel* NADH dehydrogenase activity of CI and protein

864   silver staining were performed as previously described (Pineau et al., 2008). Gels were

865   electroblotted onto nitrocellulose membranes for SDS-PAGE and PVDF for BN-PAGE.

866   Immunodetections were performed using wheat anti-NAD9 antibody (gift from J.M.

867   Grienenberger, IBPC, Strasbourg, France), anti-CA2 antibody directed against the C-terminal

868   half of the mitochondrial carbonic anhydrase 2 (*At1g47260*) from Arabidopsis (gift from E.

869   Zabaleta), and mice monoclonal *S. guttatum* anti-AOX antibody (gift from A.H. Millar).

870   Immuno-signals were visualized by ECL according to manufacturer's instructions (Roche

871   Diagnostics).

872

873   **Mini-preparations of Percoll-purified leaf mitochondria**

874   One gram of fresh material was used to obtain crude leaf mitochondrial preparations, as

875   described in Vidal et al. (2007). Mitochondria were further purified on a three-layer Percoll

876   gradient (13%, 25%, and 45% (w/v) Percoll) preformed in 2mL Effendorf tubes, using the

877   protocol designed for the purification of *N. sylvestris* pollen mitochondria (De Paepe et al.,

878   1993). Pyridine redox state could not be determined in mitochondrial extracts due to the

879   oxidation of preparations during Percoll purification.

880

881   **Rubisco radioisotopic assay**

882   Total Rubisco activity was determined from the rate of $^{14}CO_2$ incorporation into acid-stable

883   compounds and subsequent liquid scintillation counting of ^{14}C, according to Seemann and

884   Sharkley (1986); details are given in Supplemental Material.

885

886   **Antioxidant activities**

887   All enzymes were extracted from washed leaves in 50 mM potassium-phosphate pH 7.5. and

888   measurements of activities of glycolate oxidase (EC 1.1.3.1), catalase (EC 1.11.1.6),

889   ascorbate peroxidase (APX, EC 1.11.1.11) and glutathione reductase (GR, EC 1.6.4.2) were

890   as described in Streb et al. (1997). For APX activity, only the cytoplasmic form was

891   determined.

892

893   **Pigment contents**

894   Chlorophyll a/b contents were measured from 80% acetone extracts with extinction

895   coefficients reported in Porra (2002).

896

897   **Determination of soluble antioxidants in leaf and mitochondrial extracts**

898   Oxidized and reduced forms of glutathione, ascorbate, NAD and NADP were measured in

899   total leaf extracts or Percoll-purified mitochondrial preparations, by plate-reader assay, as

900   described in Queval and Noctor (2007b), modified in Pétriacq et al. (2012). Pyridine redox

901   state could not be determined in mitochondrial extracts due to their oxidation during Percoll

902   purification (Vidal. et al., 2007).

903

904   **Untargeted metabolomics by HILIC Mass Spectrometry**

905   Polar metabolites were detected by Hydrophobic Interaction Liquid Chromatography (HILIC)

906   coupled to Time-of-Flight Mass Spectrometry (q-TOF-MS) using a method from Paglia et al.

907   (2012) and modified in Pétriacq et al. (2016). Details are given in Supplemental Methods.

908

909 **Targeted metabolic profiling by Gas Chromatography Mass Spectrometry**

910 Gas Chromatography coupled to Time-of-Flight Mass Spectrometry (GC-TOF-MS) profiling

911 and quantitative analysis of amino acids by High Performance Liquid Chromatography

912 (HPLC), were performed as described in detail in Noctor et al. (2007) and Tcherkez et al.

913 (2010), using the isotopic facility structure of the Plateforme Metabolisme-Metabolome

914 (Orsay, France); details in supplemental material.

915 ATP contents were quantified using the ENLITEN ATP Assay System Bioluminescence

916 Detection Kit (Promega) using manufacturer's instructions.

917

918 **ROS determination**

919 *In situ* ROS detection was performed using nitroblue tetrazolium (NBT) and

920 diaminobenzidine (DAB) stains, detecting superoxide and hydrogen peroxide respectively, as

921 described in Dutilleul et al. (2003b). Room-temperature spin-trapping EPR spectroscopy was

922 carried out to measure apoplastic ROS, as described by Michelet and Krieger-Liszkay (2012);

923 details in supplemental material. Luminol chemiluminescence was performed on leaves as

924 described in Pétriacq et al., (2016). Results were calibrated using H_2O_2 as the ROS source.

925

926 **Nitrate reductase activity and nitrate determination**

927 NR activity was determined as described in Fresneau et al. (2007) on desalted extracts

928 purified with NAP-5 column (Sephadex™ G-25, GE Healthcare). Nitrate ions contents were

929 determined as in Cataldo et al. (1975). Details are given in Supplemental Material.

930

931 **Anthocyanin determination**

932 Anthocyanin content was determined according to Vanderauwera et al. (2005), and expressed

933 as OD 530/mg FW.

934

935 **Electron microscopy**

936 Leaf samples were processed as described in Hawes and Satiat-Jeunemaitre (2001). Details

937 are given in supplemental material

938

939 **Statistical Methods**

940 Significant differences ($P < 0.05$) were calculated using Student *t* test.

941

Accession numbers

943 Sequence data from this article can be found in the EMBL/GenBank data libraries under

944 accession number(s) *At1g16700* and *At1g79010* and in Supplemental Table 1.

945
946
947 **SUPPLEMENTAL MATERIAL**

948 **List of Supplemental Methods:** Metabolomic measurements**,** Rubisco radioisotopic assay**,**

949 detection of ROS content**,** Nitrate determination**,** Electron Microscopy HILICS Analyses

950

951 **List of Supplemental Figures**

952 **Supplemental Figure S1.** Resolution by two-dimensional (2D) BN-SDS PAGE of root

953 membrane proteins of Col-0 and of the *ndufs8.1 ndufs8.2* double mutant

954 **Supplemental Figure S2.** Electron microscopy of mitochondria in Col-0 and *ndufs8.1*

955 *ndufs8.2* leaves.

956 **Supplemental Figure S3.** Phenotypes of *ndufs8.1 and ndufs8.2 s*ingle mutants, the *ndufs8.1*

957 *ndufs8.2* double mutant and the *ndufs4* mutant

958 **Supplemental Figure S4.** Col-0, *ndufs8.1 ndufs8.2* and *ndufs4* plants grown in SD and LD

959 conditions

960 **Supplemental Figure S5.** Dimensions of leaf cells of Col-0 and *ndufs8.1 ndufs8.2 plants* in

961 SD and LD condition

962 **Supplemental Figure S6**. Micrographs of chloroplast ultrastructure in Col-0 and *ndufs8.1*

963 *ndufs8.2* plants

964 **Supplemental Figure S7.** Changes in contents of sugars and TCA derivatives in Col-0 and

965 *ndufs8.1 ndufs8.2* plants during the day/night cycle analysed using GC-MS

966 **Supplemental Figure S8.** Changes in contents of amino acids in Col-0 and *ndufs8.1 ndufs8.2*

967 plants during the day/night cycle analysed by GC-MS (part 1)

968 **Supplemental Figure S9.** Changes in contents of amino acids in Col-0 and *ndufs8.1 ndufs8.2*

969 plants during the day/night cycle analysed by GC-MS (part 2)

970 **Supplemental Figure S10.** Heat-map and hierarchical clustering (cosine correlation) of

971 metabolites found to be significant with respect to photoperiod (SD/LD) in a two-way

972 ANOVA (GC-MS metabolomics)

973 **Supplemental Figure S11.** Metabolomic pattern in Col-0 and *ndufs8.1 ndufs8.2* plants and

974 photoperiod × genotype interaction

40

975 **Supplemental Figure S12.** HPLC quantitation of amino acids in Col-0 and *ndufs8.1 ndufs8.2*

976 leaves

977 **Supplemental Figure S13**. Transcriptional analysis of TCA-related enzymes in Col-0 and

978 *ndufs8.1 ndufs8.2* leaves

979 **Supplemental Figure S14.** Gas exchange measurements of Col-0 and *ndufs8.1 ndufs8.2*

980 plants maintained under SD and LD conditions

981 **Supplemental Figure S15.** *In situ* detection of leaf superoxide and hydrogen peroxide in Col-

982 0 and *ndufs8.1 ndufs8.2* plants grown under LD and SD conditions

983 **Supplemental Figure S16.** Transcriptional analysis of redox enzymes in Col-0 and *ndufs8.1*

984 *ndufs8.2* plants under various illumination conditions

985 **Supplemental Figure S17.** Cellular antioxidant activities and anthocyanin contents of Col-0

986 and *ndufs8.1 ndufs8.2* mutant plants maintained under SD and LD conditions

987

988 **List of Supplemental   Tables:**

989 **Supplemental Table 1.** Sequences of primers and accession numbers of genes used in this

990 study

991

992 **Acknowledgements**

998

999 **LEGENDS TO FIGURES**

1000

1001 **Figure 1. Molecular characterization of single and double insertion mutants affected in**

1002 **the two Arabidopsis genes encoding the NDUFS8 subunit of Complex I**

1003 A, gene structure and sites of insertion of T-DNA in *ndufs8.1* (*At1g79010*) and *ndufs8.2*

1004 (*At1g16700*) genes (arrows). B, electrophoresis of RT-PCR products using *NDUFS8.1*and

1005 *NDUFS8.2*specific primers in the WT (Col-0), *ndufs8.1* and *ndufs8.2* single mutants, and the

1006 *ndufs8.1 ndufs8.2* double mutant. C, RT-qPCR analysis of *NDUFS8.1* and *NDUFS8.1* genes

1007   in the WT (Col-0), the *ndufs8.1* and *ndufs8.2* single mutants and the *ndufs8.1 ndufs8.2* double

1008   mutant, using *ACT2* as a reference. Data are means + SE of 3 independent measurements.

1009

1010   **Figure 2. Complex I assembly/activity in Col-0 and single and double mutants for the**

1011   **NDUFS8 subunit**

1012   Membrane proteins extracted from leaves of Col-0 (1), single *ndufs8.1 (2), ndufs8.2 (3)* and

1013   *ndufs8.1 ndufs8.2* double *(4)* mutants were solubilized with digitonin that preserves assembly

1014   of super-complexes and resolved by BN-PAGE on 4/13% gradient acrylamide gels. After

1015   migration, gels were stained for CI activity using NADH/NBT or blotted on PVDF

1016   membranes for immuno-detection studies.

1017   - Left: in-gel NADH/NBT-stained leaf proteins; CI and the CI/III super complex (purple

1018   signals, red arrows), detected in Col-0 and in both *ndufs8.1-* and *ndufs8.2* single mutants, are

1019   absent in the double mutant. The PSI complex originated from thylakoid membranes is

1020   indicated by an arrowhead (see Pineau et al., 2008).

1021   - Middle: the anti-NAD9 immuno-signal revealed at the level of CI in the WT and in both

1022   *ndufs8.1* and *ndufs8.2* single mutants, is not detected in the *ndufs8.1 ndufs8.2* double mutant.

1023   - Right: accumulation of Complex IV using anti-COX2 antibody (bottom of the gel) is similar

1024   in all genotypes.

1025

1026   **Figure 3. Respiratory pathways and mitochondrial proteins in Col-0 and *ndufs8.1***

1027   ***ndufs8.2* mutant**

1028   A, Respiration rates of Col-0 and the *ndufs8.1 ndufs8.2* double mutant were determined by

1029   oxygen discrimination. Measurements were performed on plants grown in controlled

1030   chambers in under 12h/12h, day/night; vt: total oxygen uptake; vcyt: cytochrome oxidase

1031   activity; valt: alternative oxidase activity (AOX); τ: partition to the AOX pathway. Data are

1032   means +SE of measurements performed on at least 3 different plants; * indicate significant

1033   differences between WT and mutant.

1034   B, AOX capacity: % of cyanide resistant respiration in leaf tissues, determined as in Florez-

1035   Sarasa et al. (2009). Data are means + SE of measurements performed on at least 3 different

1036   plants; * indicate significant difference between Col-0 and mutant.

1037   C, Immuno-detection of mitochondrial (mt) proteins on total leaf membranes (tot mb, left)

1038   and mitochondrial membranes (mt mb, right); * indicates mitochondrial specific immuno-

1039   signals. The experiment was performed at least 3 times with similar results.

1040

1041 **Figure 4. Growth comparisons of Col-0, *ndufs8.1 ndufs8.2* and *ndufs4* plants in the short**

1042 **day (SD) to long day (LD) transfer experiment**

1043 **A**, Col-0 and mutant plants (*ndufs8.1 ndufs8.2* and *ndufs4)* were initially grown in controlled

1044 rooms under SD to achieve a similar development (8-9 leaf state, SD0), then transferred to

1045 LD for 3 days (LD3) or 6 days (LD6).

1046 **B**, Histograms of fresh weight (FW, mg) of SD0, SD6 and LD6 plants in Col-0 (black),

1047 *ndufs8.1 ndufs8.2* (grey) and *ndufs4* (white). Data are means +SE of measurements on at least

1048 8 different plants in all genotypes. Differences between mutant and Col-0 values are much

1049 higher in LD than in SD condition; * indicates significant differences between mutants and

1050 Col-0 according to Student *t* test.

1051 **C**, LD/SD ratios of plant biomass (FW) in Col-0 (black), *ndufs8.1 ndufs8.2* (grey) and *ndufs4*

1052 (white) plants; asterisks indicate significant differences between mutants and Col-0.

1053

1054 **Figure 5. Untargeted metabolomics by HILIC-qTOF-MS**

1055 Multivariate analyses of number anions (ESI$^-$) and cations (ESI$^+$) detected by HILIC-qTOF-

1056 MS from Col-0 (squares), *ndufs8.1 ndufs8.2* (triangles) and *ndufs4* (circles) plants grown in

1057 short days (SD, white symbols) or long days (LD, grey symbols) *(n* = 3)*. **A**, un-supervised

1058 principal component analysis (PCA) displaying the overall metabolic trends between samples.

1059 Variances are given into brackets. **B**, hierarchical clustering analysis (HCA) showing

1060 metabolic relationships between genotypes and photoperiods (Single linkage, tree sorted by

1061 size).

1062

1063 **Figure 6. GC-MS determination of metabolites in Col-0, *ndufs8.1 ndufs8.2* and *ndufs4***

1064 **plants**

1065 Leaves were sampled from SD6/LD6 plants at the middle of the day period; analyte contents

1066 are expressed in relative units; black columns: Col-0; grey columns: *ndufs8.1 ndufs8.2;* white

1067 columns: *ndufs4*

1068

1069 **Figure 7. Heat-map and hierarchical clustering (cosine correlation) of metabolites found**

1070 **to be significant with respect to genotype (in a two-way ANOVA GC-MS metabolomics)**

1071 Col-0 (col) and *ndufs8.1 ndufs8.2* (mut) leaves were sampled from SD3/LD3 plants at the

1072 middle of the light period and from SD6/LD6 plants both at the middle of the light period and

1073 at the end of the night period (dark). Metabolomics analyses were carried out 3 times (*i.e.*, 3

1074 biological replicates). Relative metabolite contents are represented as mean-centered values

1075   with a color scale (blue, low content; red, high content). Numbers close to metabolite names

1076   refer to individual analytes associated with the metabolite of interest.

1077

1078   **Figure 8. Analysis of growth-related parameters in Col-0 and *ndufs8.1 ndufs8.2***

1079   Leaves were sampled from Col-0 and *ndufs8.1 ndufs8.2*plants at the middle of the light period

1080   at the day 12 time point; SD: short day; LD: long day.

1081   A, Carbon exchange-related parameters determined on leaves of 2-3 month old rosette plants

1082   at the same developmental stage. Carboxylation efficiency (ce, µmol CO_2 m^{-2} s^{-1}); stomatal

1083   conductance for CO_2 (*gs*, mol $m^{-2} s^{-1}$) calculated at growth illumination; Rubisco capacity (*in*

1084   *vitro* measured maximum activity, nmol CO_2 min^{-1} mg $prot^{-1}$); chlorophyll a/chlorophyll b

1085   ratios; night respiration (Rn, CO_2, µmol CO_2 m^{-2} s^{-1}) and total leaf ATP (nmol g^{-1} FW) are

1086   means + SE of 3-6 measurements on different plants. Different letters indicate significant

1087   differences according to Student *t* test.

1088   B, Nitrogen assimilation-related parameters. Total leaf free amino acids (µmol g^{-1} FW)

1089   determined from HPLC quantification (see Supplemental Figure S12); soluble proteins (mg g^-

1090 ^{1} FW); total N content (%); NR capacity (maximum activity, µmol NO_2^- h^{-1} mg^{-1} prot); RT-

1091   qPCR analysis of the major nitrate reductase gene (*NR2,* relative expression to *ACT2*); nitrate

1092   contents (µmol g^{-1} FW). Data are means +SE of 3-6 measurements on different plants.

1093   Different letters indicate significant differences according to Student t test.

1094   C, RT-qPCR analysis of *TOR2/LST8* genes of the nutrient-dependent TOR pathway using

1095   ACT2 as a reference. Data are means +SE of 3-6 measurements on different plants. Different

1096   letters indicate significant differences according to Student t test.

1097   D, RT-qPCR analysis of CCA1/LHY clock regulators. Data are means +SE of 6

1098   measurements on different plants. Different letters indicate significant differences according

1099   to Student t test.

1100

1101   **Figure 9. ROS content and expression levels of antioxidant enzymes in Col-0 and**

1102   ***ndufs8.1 ndufs8.2* plants maintained under SD and LD condition**

1103   A, Typical EPR spectroscopy spectra, performed on leaf disks sampled from SD12/LD12

1104   plants, as described in Michelet and Krieger-Liszkay (2012).

1105   B, Total soluble ROS pools (H_2O_2 equivalents) detected by luminol chemiluminescence in

1106   leaves sampled from SD12/LD12 plants at the middle of the light period (left) and at the end

1107   of the dark period (right). Data are means +SE of measurements on 4-6 different plants.

1108   Different letters indicate significant differences according to Student *t* test.

1109   C, RT-qPCR analysis of redox enzymes of leaves sampled from SD12/LD12 plants at the

1110   middle of the light period; *ACT2* was used as a reference. Data are means +SE of

1111   measurements on 3-6 different plants. Different letters indicate statistical differences

1112   according to Student *t* test.

1113

1114   **Figure 10. Pools of foliar redox buffers and co-factors in Col-0, *ndufs8.1 ndufs8.2* and**

1115   ***ndufs4* plants**

1116   Leaves were sampled from SD6/LD6 plants at the middle of the day period. Black columns:

1117   Col-0; dark grey columns: *ndufs8.1 ndufs8.2*; white columns: *ndufs4*

1118   A, Redox buffers

1119   - Left: total leaf content of reduced and oxidized (top, light grey) forms of glutathione (nmol

1120 g^{-1} FW) and ascorbate (µmol g^{-1} FW). Redox state (% of oxidised forms) is indicated on top

1121   of the histograms. Data are means +SE from at least 4 extracts from different plants;

1122   * indicate significant differences (P<0.05) between WT and mutant total pools according to

1123   Student t test; ° indicate significant differences between SD and LD values for the same

1124   genotype.

1125   - Right: LD/SD ratios in the three genotypes.

1126   B, Redox co-factors

1127   - Left Total leaf content of oxidized and reduced (top, light grey) forms of NAD(H) and

1128   NAD(P)H (nmol g^{-1} FW); NAD (P)+/NAD(P)H ratios are indicated on top of the histograms.

1129   Results are means +SE of 8 extracts from different plants; * indicates significant differences

1130   (P<0.05) between WT and mutant total pools according to Student t test; ° indicates

1131   significant differences between SD and LD values for the same genotype.

1132   - Right: LD/SD ratios in the three genotypes.

1133

1134   **Figure 11. Pools of mitochondrial NAD$^+$ and transcriptional analysis of NAD$^+$**

1135   **biosynthetic genes**

1136   In all experiments, leaves were sampled from SD12/LD12 Col-0 and *ndufs8.1 ndufs8.2* plants

1137   at the middle of the day period.

1138   A, NAD$^+$ (nmol g^{-1} FW) contents of mitochondrial preparations. Results are means +SE of 3

1139   extracts from different plants.

1140   B, RT-qPCR analyses of NAD$^+$ biosynthetic genes were carried out using *ACT2* as a

1141   reference.   Aspartate   oxidase   (*AO*),   quinolinate   synthase   (*QS*),   quinolinate

1142   phosphoribosyltransferase (*QPT*), nicotinate mononucleotide adenylyltransferase (*NaMNAT*),

45

1143   NAD synthetase (*NADS*) and nicotinate phosphoribosyltranferase 2, 4 (*NaPT2, 4*) and Poly-

1144   ADP-ribose polymerase2 *(PARP2)*. Results are means + SE of at least 6 extracts from

1145   different plants. Different letters indicate significant differences according to Student *t* test.

1146

1147

Parsed Citations

Ahmad M, Lin C, Cashmore AR (1995) Mutations throughout an Arabidopsis blue-light photoreceptor impair blue-light-responsive anthocyanin accumulation and inhibition of hypocotyl elongation. Plant J 8: 653-658
Pubmed: Author and Title
CrossRef: Author and Title
Google Scholar: Author Only Title Only Author and Title

Alonso JM, Stepanova AN, Leisse TJ, Kim CJ, Chen H, Shinn P, Stevenson DK, Zimmerman J, Barajas P, Cheuk R, et al (2003) Genome-wide insertional mutagenesis of Arabidopsis thaliana. Science 301: 653-657
Pubmed: Author and Title
CrossRef: Author and Title
Google Scholar: Author Only Title Only Author and Title

Araújo WL, Nunes-Nesi A, Nikoloski Z, Sweetlove LJ, Fernie AR (2012) Metabolic control and regulation of the tricarboxylic acid cycle in photosynthetic and heterotrophic plant tissues. Plant Cell Environ 35: 1-21
Pubmed: Author and Title
CrossRef: Author and Title
Google Scholar: Author Only Title Only Author and Title

Becker B, Holtgrefe S, Jung S, Wunrau C, Kandlbinder A, Baier M, Dietz K-J, Backhausen JE, Scheibe R (2006) Influence of the photoperiod on redox regulation and stress responses in Arabidopsis thaliana L. (Heynh.) plants under long- and short-day conditions. Planta 224: 380-393
Pubmed: Author and Title
CrossRef: Author and Title
Google Scholar: Author Only Title Only Author and Title

Brangeon J, Sabar M, Gutierres S, Combettes B, Bove J, Gendy C, Chétrit P, Des Francs-Small CC, Pla M, Vedel F, et al (2000) Defective splicing of the first nad4 intron is associated with lack of several complex I subunits in the Nicotiana sylvestris NMS1 nuclear mutant. Plant J 21: 269-280
Pubmed: Author and Title
CrossRef: Author and Title
Google Scholar: Author Only Title Only Author and Title

op den Camp RGL, Przybyla D, Ochsenbein C, Laloi C, Kim C, Danon A, Wagner D, Hideg E, Göbel C, Feussner I, et al (2003) Rapid induction of distinct stress responses after the release of singlet oxygen in Arabidopsis. Plant Cell 15: 2320-2332
Pubmed: Author and Title
CrossRef: Author and Title
Google Scholar: Author Only Title Only Author and Title

Cataldo DA, Maroon M, Schrader LE, Youngs VL (1975) Rapid colorimetric determination of nitrate in plant tissue by nitration of salicylic acid. Commun Soil Sci Plant Anal 6: 71-80
Pubmed: Author and Title
CrossRef: Author and Title
Google Scholar: Author Only Title Only Author and Title

Cohen S, Zmudjak M, Colas des Francs-Small C, Malik S, Shaya F, Keren I, Belausov E, Many Y, Brown GG, Small I, et al (2014) nMAT4, a maturase factor required for nad1 pre-mRNA processing and maturation, is essential for holocomplex I biogenesis in Arabidopsis mitochondria. Plant J 78: 253-268
Pubmed: Author and Title
CrossRef: Author and Title
Google Scholar: Author Only Title Only Author and Title

Colas des Francs-Small C, Small I (2014) Surrogate mutants for studying mitochondrially encoded functions. Biochimie 100: 234-242
Pubmed: Author and Title
CrossRef: Author and Title
Google Scholar: Author Only Title Only Author and Title

De Paepe R, Chétrit P, Vitart V, Ambard-Bretteville F, Prat D, Vedel F (1990) Several nuclear genes control both male sterility and mitochondrial protein synthesis in Nicotiana sylvestris protoclones. Mol Gen Genet 222: 206-210
Pubmed: Author and Title
CrossRef: Author and Title
Google Scholar: Author Only Title Only Author and Title

De Paepe R, Forchioni A, Chétrit P, Vedel F (1993) Specific mitochondrial proteins in pollen: presence of an additional ATP synthase beta subunit. Proc Natl Acad Sci U S A 90: 5934-5938
Pubmed: Author and Title
CrossRef: Author and Title
Google Scholar: Author Only Title Only Author and Title

Djebbar R, Rzigui T, Pétriacq P, Mauve C, Priault P, Fresneau C, De Paepe M, Florez-Sarasa I, Benhassaine-Kesri G, Streb P, et al (2012) Respiratory complex I deficiency induces drought tolerance by impacting leaf stomatal and hydraulic conductances. Planta 235: 603-614
Pubmed: Author and Title
CrossRef: Author and Title
Google Scholar: Author Only Title Only Author and Title

Dutilleul C, Driscoll S, Cornic G, De Paepe R, Foyer CH, Noctor G (2003a) Functional mitochondrial complex I is required by tobacco leaves for optimal photosynthetic performance in photorespiratory conditions and during transients. Plant Physiol 131:

264-275

Pubmed: Author and Title
CrossRef: Author and Title
Google Scholar: Author Only Title Only Author and Title

Dutilleul C, Garmier M, Noctor G, Mathieu C, Chétrit P, Foyer CH, De Paepe R (2003b) Leaf mitochondria modulate whole cell redox homeostasis, set antioxidant capacity, and determine stress resistance through altered signaling and diurnal regulation. Plant Cell 15: 1212

Pubmed: Author and Title
CrossRef: Author and Title
Google Scholar: Author Only Title Only Author and Title

Dutilleul C, Lelarge C, Prioul J-L, De Paepe R, Foyer CH, Noctor G (2005) Mitochondria-driven changes in leaf NAD status exert a crucial influence on the control of nitrate assimilation and the integration of carbon and nitrogen metabolism. Plant Physiol 139: 64-78

Pubmed: Author and Title
CrossRef: Author and Title
Google Scholar: Author Only Title Only Author and Title

Efremov RG, Baradaran R, Sazanov LA (2010) The architecture of respiratory complex I. Nature 465: 441-445

Pubmed: Author and Title
CrossRef: Author and Title
Google Scholar: Author Only Title Only Author and Title

Florez-Sarasa ID, Bouma TJ, Medrano H, Azcon-Bieto J, Ribas-Carbo M (2007) Contribution of the cytochrome and alternative pathways to growth respiration and maintenance respiration in Arabidopsis thaliana. Physiol Plant 129: 143-151

Pubmed: Author and Title
CrossRef: Author and Title
Google Scholar: Author Only Title Only Author and Title

Florez-Sarasa I, Ostaszewska M, Galle A, Flexas J, Rychter AM, Ribas-Carbo M (2009) Changes of alternative oxidase activity, capacity and protein content in leaves of Cucumis sativus wild-type and MSC16 mutant grown under different light intensities. Physiol Plant 137: 419-426

Pubmed: Author and Title
CrossRef: Author and Title
Google Scholar: Author Only Title Only Author and Title

Foyer CH, Noctor G (2011) Ascorbate and glutathione: the heart of the redox hub. Plant Physiol 155: 2

Pubmed: Author and Title
CrossRef: Author and Title
Google Scholar: Author Only Title Only Author and Title

Foyer, C. H., Noctor, G., & Hodges, M. (2011). Respiration and nitrogen assimilation: targeting mitochondria-associated metabolism as a means to enhance nitrogen use efficiency. J Exp Bot 62: 1467-1482

Pubmed: Author and Title
CrossRef: Author and Title
Google Scholar: Author Only Title Only Author and Title

Fresneau C, Ghashghaie J, Cornic G (2007) Drought effect on nitrate reductase and sucrose-phosphate synthase activities in wheat (Triticum durum L.): role of leaf internal CO_2. J Exp Bot 58: 2983-2992

Pubmed: Author and Title
CrossRef: Author and Title
Google Scholar: Author Only Title Only Author and Title

Fromm, S., Göing, J., Lorenz, C., Peterhänsel, C., & Braun, H. P. (2016). Depletion of the "gamma-type carbonic anhydrase-like" subunits of complex I affects central mitochondrial metabolism in Arabidopsis thaliana. Biochimica et Biophysica Acta (BBA)-Bioenergetics 1857: 60-71

Pubmed: Author and Title
CrossRef: Author and Title
Google Scholar: Author Only Title Only Author and Title

Fukushima A, Kusano M, Nakamichi N, Kobayashi M, Hayashi N, Sakakibara H, Mizuno T, Saito K (2009) Impact of clock-associated Arabidopsis pseudo-response regulators in metabolic coordination. Proc Natl Acad Sci U S A 106: 7251-7256

Pubmed: Author and Title
CrossRef: Author and Title
Google Scholar: Author Only Title Only Author and Title

Galle A, Florez-Sarasa I, Thameur A, De Paepe R, Flexas J, Ribas-Carbo M (2010) Effects of drought stress and subsequent rewatering on photosynthetic and respiratory pathways in Nicotiana sylvestris wild type and the mitochondrial complex I-deficient CMSII mutant. J Exp Bot 61: 765-775

Pubmed: Author and Title
CrossRef: Author and Title
Google Scholar: Author Only Title Only Author and Title

Gibon Y, Bläsing OE, Palacios-Rojas N, Pankovic D, Hendriks JHM, Fisahn J, Höhne M, Günther M, Stitt M (2004) Adjustment of diurnal starch turnover to short days: depletion of sugar during the night leads to a temporary inhibition of carbohydrate utilization, accumulation of sugars and post-translational activation of ADP-glucose pyrophosphorylase in the following light period. Plant J 39: 847-862

Pubmed: Author and Title
CrossRef: Author and Title

Google Scholar: Author Only Title Only Author and Title

Gibon Y, Pyl E-T, Sulpice R, Lunn JE, Höhne M, Günther M, Stitt M (2009) Adjustment of growth, starch turnover, protein content and central metabolism to a decrease of the carbon supply when Arabidopsis is grown in very short photoperiods. Plant Cell Environ 32: 859-874
Pubmed: Author and Title
CrossRef: Author and Title
Google Scholar: Author Only Title Only Author and Title

Gupta KJ, Shah JK, Brotman Y, Jahnke K, Willmitzer L, Kaiser WM, Bauwe H, Igamberdiev AU (2012). Inhibition of aconitase by nitric oxide leads to induction of the alternative oxidase and to a shift of metabolism towards biosynthesis of amino acids. J Exp Bot. 63:1773-84
Pubmed: Author and Title
CrossRef: Author and Title
Google Scholar: Author Only Title Only Author and Title

Gutierres S, Sabar M, Lelandais C, Chetrit P, Diolez P, Degand H, Boutry M, Vedel F, de Kouchkovsky Y, De Paepe R (1997) Lack of mitochondrial and nuclear-encoded subunits of complex I and alteration of the respiratory chain in Nicotiana sylvestris mitochondrial deletion mutants. Proc Natl Acad Sci U S A 94: 3436-3441
Pubmed: Author and Title
CrossRef: Author and Title
Google Scholar: Author Only Title Only Author and Title

Giraud, E., Ng, S., Carrie, C., Duncan, O., Low, J., Lee, C. P., ... & Whelan, J. (2010). TCP transcription factors link the regulation of genes encoding mitochondrial proteins with the circadian clock in Arabidopsis thaliana. Plant Cell 22: 3921-3934
Pubmed: Author and Title
CrossRef: Author and Title
Google Scholar: Author Only Title Only Author and Title

Guy RD, Berry JA, Fogel ML, Hoering TC (1989) Differential fractionation of oxygen isotopes by cyanide-resistant and cyanide-sensitive respiration in plants. Planta 177: 483-491
Pubmed: Author and Title
CrossRef: Author and Title
Google Scholar: Author Only Title Only Author and Title

Hager J, Pellny TK, Mauve C, Lelarge-Trouverie C, De Paepe R, Foyer CH, Noctor G (2010) Conditional modulation of NAD levels and metabolite profiles in Nicotiana sylvestris by mitochondrial electron transport and carbon/nitrogen supply. Planta 231: 1145-1157
Pubmed: Author and Title
CrossRef: Author and Title
Google Scholar: Author Only Title Only Author and Title

Hashida SN, Takahashi H, Uchimiya H (2009) The role of NAD biosynthesis in plant development and stress responses. Ann Bot 103: 819-824
Pubmed: Author and Title
CrossRef: Author and Title
Google Scholar: Author Only Title Only Author and Title

Hawes CR, Satiat-Jeunemaitre B, eds (2001) Plant cell biology: a practical approach, 2nd ed. Oxford University Press, Oxford?; New York
Pubmed: Author and Title
CrossRef: Author and Title
Google Scholar: Author Only Title Only Author and Title

Haydon MJ, Román Á, Arshad W (2015) Nutrient homeostasis within the plant circadian network. Front Plant Sci 6: 299
Pubmed: Author and Title
CrossRef: Author and Title
Google Scholar: Author Only Title Only Author and Title

Heldt H. W. Plant Biochemistry, 3rd edn. (Elsevier Academic Press, 2005).

Huang S, Van Aken O, Schwarzländer M, Belt K, Millar AH (2016) The Roles of Mitochondrial Reactive Oxygen Species in Cellular Signaling and Stress Response in Plants. Plant Physiol 171:1551-1559
Pubmed: Author and Title
CrossRef: Author and Title
Google Scholar: Author Only Title Only Author and Title

Hurd TR, Collins Y, Abakumova I, Chouchani ET, Baranowski B, Fearnley IM, Prime TA, Murphy MP, James AM (2012) Inactivation of pyruvate dehydrogenase kinase 2 by mitochondrial reactive oxygen species. J Biol Chem 287: 35153-35160
Pubmed: Author and Title
CrossRef: Author and Title
Google Scholar: Author Only Title Only Author and Title

Igamberdiev AU, Gardeström P (2003) Regulation of NAD- and NADP-dependent isocitrate dehydrogenases by reduction levels of pyridine nucleotides in mitochondria and cytosol of pea leaves. Biochim Biophys Acta 1606: 117-125
Pubmed: Author and Title
CrossRef: Author and Title
Google Scholar: Author Only Title Only Author and Title

Karpova OV, Kuzmin EV, Elthon TE, Newton KJ (2002) Differential expression of alternative oxidase genes in maize mitochondrial

mutants. Plant Cell 14: 3271-3284

Pubmed: Author and Title
CrossRef: Author and Title
Google Scholar: Author Only Title Only Author and Title

Karpova OV, Newton KJ (1999) A partially assembled complex I in NAD4-deficient mitochondria of maize. Plant J 17: 511-521

Pubmed: Author and Title
CrossRef: Author and Title
Google Scholar: Author Only Title Only Author and Title

Katoh A, Uenohara K, Akita M, Hashimoto T (2006) Early steps in the biosynthesis of NAD in Arabidopsis start with aspartate and occur in the plastid. Plant Physiol 141: 851-857

Pubmed: Author and Title
CrossRef: Author and Title
Google Scholar: Author Only Title Only Author and Title

Keren I, Tal L, des Francs-Small CC, Araújo WL, Shevtsov S, Shaya F, Fernie AR, Small I, Ostersetzer-Biran O (2012) nMAT1, a nuclear-encoded maturase involved in the trans-splicing of nad1 intron 1, is essential for mitochondrial complex I assembly and function. Plant J 71: 413-426

Pubmed: Author and Title
CrossRef: Author and Title
Google Scholar: Author Only Title Only Author and Title

Klodmann J, Sunderhaus S, Nimtz M, Jänsch L, Braun H-P (2010) Internal architecture of mitochondrial complex I from Arabidopsis thaliana. Plant Cell 22: 797-810

Pubmed: Author and Title
CrossRef: Author and Title
Google Scholar: Author Only Title Only Author and Title

Koussevitzky S, Suzuki N, Huntington S, Armijo L, Sha W, Cortes D, Shulaev V, Mittler R (2008) Ascorbate peroxidase 1 plays a key role in the response of Arabidopsis thaliana to stress combination. J Biol Chem 283: 34197-34203

Pubmed: Author and Title
CrossRef: Author and Title
Google Scholar: Author Only Title Only Author and Title

Kühn K, Obata T, Feher K, Bock R, Fernie AR, Meyer EH (2015) Complete Mitochondrial Complex I Deficiency Induces an Up-Regulation of Respiratory Fluxes That Is Abolished by Traces of Functional Complex I. Plant Physiol 168: 1537-1549

Pubmed: Author and Title
CrossRef: Author and Title
Google Scholar: Author Only Title Only Author and Title

Leman G, Gueguen N, Desquiret-Dumas V, Kane MS, Wettervald C, Chupin S, Chevrollier A, Lebre A-S, Bonnefont J-P, Barth M, et al (2015) Assembly defects induce oxidative stress in inherited mitochondrial complex I deficiency. Int J Biochem Cell Biol 65: 91-103

Pubmed: Author and Title
CrossRef: Author and Title
Google Scholar: Author Only Title Only Author and Title

Lepistö A, Rintamäki E (2012) Coordination of plastid and light signaling pathways upon development of Arabidopsis leaves under various photoperiods. Mol Plant 5: 799-816

Pubmed: Author and Title
CrossRef: Author and Title
Google Scholar: Author Only Title Only Author and Title

Liu Y-J, Nunes-Nesi A, Wallström SV, Lager I, Michalecka AM, Norberg FEB, Widell S, Fredlund KM, Fernie AR, Rasmusson AG (2009) A redox-mediated modulation of stem bolting in transgenic Nicotiana sylvestris differentially expressing the external mitochondrial NADPH dehydrogenase. Plant Physiol 150: 1248-1259

Pubmed: Author and Title
CrossRef: Author and Title
Google Scholar: Author Only Title Only Author and Title

Liu, Y., He, J., Chen, Z., Ren, X., Hong, X., & Gong, Z. (2010). ABA overly-sensitive 5 (ABO5), encoding a pentatricopeptide repeat protein required for cis-splicing of mitochondrial nad2 intron 3, is involved in the abscisic acid response in Arabidopsis. The Plant Journal 63: 749-765

Pubmed: Author and Title
CrossRef: Author and Title
Google Scholar: Author Only Title Only Author and Title

de Longevialle AF, Meyer EH, Andrés C, Taylor NL, Lurin C, Millar AH, Small ID (2007) The pentatricopeptide repeat gene OTP43 is required for trans-splicing of the mitochondrial nad1 Intron 1 in Arabidopsis thaliana. Plant Cell 19: 3256-3265

Pubmed: Author and Title
CrossRef: Author and Title
Google Scholar: Author Only Title Only Author and Title

Marienfeld JR, Newton KJ (1994) The maize NCS2 abnormal growth mutant has a chimeric nad4-nad7 mitochondrial gene and is associated with reduced complex I function. Genetics 138: 855-863

Pubmed: Author and Title
CrossRef: Author and Title
Google Scholar: Author Only Title Only Author and Title

Meyer EH, Solheim C, Tanz SK, Bonnard G, Millar AH (2011) Insights into the composition and assembly of the membrane arm of plant complex I through analysis of subcomplexes in Arabidopsis mutant lines. J Biol Chem 286: 26081-26092
Pubmed: Author and Title
CrossRef: Author and Title
Google Scholar: Author Only Title Only Author and Title

Meyer EH, Tomaz T, Carroll AJ, Estavillo G, Delannoy E, Tanz SK, Small ID, Pogson BJ, Millar AH (2009) Remodeled respiration in ndufs4 with low phosphorylation efficiency suppresses Arabidopsis germination and growth and alters control of metabolism at night. Plant Physiol 151: 603-619
Pubmed: Author and Title
CrossRef: Author and Title
Google Scholar: Author Only Title Only Author and Title

Michalecka AM, Svensson AS, Johansson FI, Agius SC, Johanson U, Brennicke A, Binder S, Rasmusson AG (2003) Arabidopsis genes encoding mitochondrial type II NAD(P)H dehydrogenases have different evolutionary origin and show distinct responses to light. Plant Physiol 133: 642-652
Pubmed: Author and Title
CrossRef: Author and Title
Google Scholar: Author Only Title Only Author and Title

Michelet L, Krieger-Liszkay A (2012) Reactive oxygen intermediates produced by photosynthetic electron transport are enhanced in short-day grown plants. Biochim Biophys Acta 1817: 1306-1313
Pubmed: Author and Title
CrossRef: Author and Title
Google Scholar: Author Only Title Only Author and Title

Miwa S, Jow H, Baty K, Johnson A, Czapiewski R, Saretzki G, Treumann A, von Zglinicki T (2014) Low abundance of the matrix arm of complex I in mitochondria predicts longevity in mice. Nat Commun 5: 3837
Pubmed: Author and Title
CrossRef: Author and Title
Google Scholar: Author Only Title Only Author and Title

Møller IM (2001) PLANT MITOCHONDRIA AND OXIDATIVE STRESS: Electron Transport, NADPH Turnover, and Metabolism of Reactive Oxygen Species. Annu Rev Plant Physiol Plant Mol Biol 52: 561-591
Pubmed: Author and Title
CrossRef: Author and Title
Google Scholar: Author Only Title Only Author and Title

Moreau M, Azzopardi M, Clément G, Dobrenel T, Marchive C, Renne C, Martin-Magniette M-L, Taconnat L, Renou J-P, Robaglia C, et al (2012) Mutations in the Arabidopsis homolog of LST8/GβL, a partner of the target of Rapamycin kinase, impair plant growth, flowering, and metabolic adaptation to long days. Plant Cell 24: 463-481
Pubmed: Author and Title
CrossRef: Author and Title
Google Scholar: Author Only Title Only Author and Title

Mouchiroud L, Houtkooper RH, Moullan N, Katsyuba E, Ryu D, Cantó C, Mottis A, Jo Y-S, Viswanathan M, Schoonjans K, et al (2013) The NAD(+)/Sirtuin Pathway Modulates Longevity through Activation of Mitochondrial UPR and FOXO Signaling. Cell 154: 430-441
Pubmed: Author and Title
CrossRef: Author and Title
Google Scholar: Author Only Title Only Author and Title

Nagel DH, Kay SA (2012) Complexity in the wiring and regulation of plant circadian networks. Curr Biol CB 22: R648-657
Pubmed: Author and Title
CrossRef: Author and Title
Google Scholar: Author Only Title Only Author and Title

Noctor G, Bergot G, Mauve C, Thominet D, Lelarge-Trouverie C, Prioul J-L (2007) A comparative study of amino acid measurement in leaf extracts by gas chromatography-time of flight-mass spectrometry and high performance liquid chromatography with fluorescence detection. Metabolomics 3: 161-174
Pubmed: Author and Title
CrossRef: Author and Title
Google Scholar: Author Only Title Only Author and Title

Noctor G, Queval G, Gakière B (2006) NAD(P) synthesis and pyridine nucleotide cycling in plants and their potential importance in stress conditions. J Exp Bot 57: 1603-1620
Pubmed: Author and Title
CrossRef: Author and Title
Google Scholar: Author Only Title Only Author and Title

O'Leary, B., Park, J., & Plaxton, W. C. (2011). The remarkable diversity of plant PEPC (phosphoenolpyruvate carboxylase): recent insights into the physiological functions and post-translational controls of non-photosynthetic PEPCs. Biochem J 436:15-34
Pubmed: Author and Title
CrossRef: Author and Title
Google Scholar: Author Only Title Only Author and Title

Paglia G, Hrafnsdóttir S, Magnúsdóttir M, Fleming RMT, Thorlacius S, Palsson BØ, Thiele I (2012) Monitoring metabolites consumption and secretion in cultured cells using ultra-performance liquid chromatography quadrupole-time of flight mass spectrometry (UPLC-Q-ToF-MS). Anal Bioanal Chem 402: 1183-1198
Pubmed: Author and Title

CrossRef: Author and Title
Google Scholar: Author Only Title Only Author and Title

Peek CB, Affinati AH, Ramsey KM, Kuo H-Y, Yu W, Sena LA, Ilkayeva O, Marcheva B, Kobayashi Y, Omura C, et al (2013) Circadian clock NAD+ cycle drives mitochondrial oxidative metabolism in mice. Science 342: 1243417
Pubmed: Author and Title
CrossRef: Author and Title
Google Scholar: Author Only Title Only Author and Title

Peek CB, Ramsey KM, Marcheva B, Bass J (2012) Nutrient sensing and the circadian clock. Trends Endocrinol Metab TEM 23: 312-318
Pubmed: Author and Title
CrossRef: Author and Title
Google Scholar: Author Only Title Only Author and Title

Pellny TK, Van Aken O, Dutilleul C, Wolff T, Groten K, Bor M, De Paepe R, Reyss A, Van Breusegem F, Noctor G, et al (2008) Mitochondrial respiratory pathways modulate nitrate sensing and nitrogen-dependent regulation of plant architecture in Nicotiana sylvestris. Plant J 54: 976-992
Pubmed: Author and Title
CrossRef: Author and Title
Google Scholar: Author Only Title Only Author and Title

Perales M, Eubel H, Heinemeyer J, Colaneri A, Zabaleta E, Braun HP (2005). Disruption of a nuclear gene encoding a mitochondrial gamma carbonic anhydrase reduces complex I and supercomplex I + III2 levels and alters mitochondrial physiology in Arabidopsis. J Mol Biol. 350:263-77
Pubmed: Author and Title
CrossRef: Author and Title
Google Scholar: Author Only Title Only Author and Title

Pétriacq P, de Bont L, Hager J, Didierlaurent L, Mauve C, Guérard F, Noctor G, Pelletier S, Renou J-P, Tcherkez G, et al (2012) Inducible NAD overproduction in Arabidopsis alters metabolic pools and gene expression correlated with increased salicylate content and resistance to Pst-AvrRpm1. Plant J 70: 650-665
Pubmed: Author and Title
CrossRef: Author and Title
Google Scholar: Author Only Title Only Author and Title

Pétriacq P, de Bont L, Tcherkez G, Gakière B (2013) NAD: not just a pawn on the board of plant-pathogen interactions. Plant Signal Behav 8: e22477
Pubmed: Author and Title
CrossRef: Author and Title
Google Scholar: Author Only Title Only Author and Title

Pétriacq P, Ton J, Patrit O, Tcherkez G, Gakière B (2016) NAD acts as an integral regulator of multiple defense layers. Plant Physiol 172: 1-15
Pubmed: Author and Title
CrossRef: Author and Title
Google Scholar: Author Only Title Only Author and Title

Pineau B, Layoune O, Danon A, De Paepe R (2008) L-galactono-1,4-lactone dehydrogenase is required for the accumulation of plant respiratory complex I. J Biol Chem 283: 32500-32505
Pubmed: Author and Title
CrossRef: Author and Title
Google Scholar: Author Only Title Only Author and Title

Pineau B, Mathieu C, Gérard-Hirne C, De Paepe R, Chétrit P (2005) Targeting the NAD7 subunit to mitochondria restores a functional complex I and a wild type phenotype in the Nicotiana sylvestris CMS II mutant lacking nad7. J Biol Chem 280: 25994-26001
Pubmed: Author and Title
CrossRef: Author and Title
Google Scholar: Author Only Title Only Author and Title

Pla M, Mathieu C, De Paepe R, Chétrit P, Vedel F (1995) Deletion of the last two exons of the mitochondrial nad7 gene results in lack of the NAD7 polypeptide in a Nicotiana sylvestris CMS mutant. Mol Gen Genet 248: 79-88
Pubmed: Author and Title
CrossRef: Author and Title
Google Scholar: Author Only Title Only Author and Title

Porra RJ (2002) The chequered history of the development and use of simultaneous equations for the accurate determination of chlorophylls a and b. Photosynth Res 73: 149-156
Pubmed: Author and Title
CrossRef: Author and Title
Google Scholar: Author Only Title Only Author and Title

Priault P, Fresneau C, Noctor G, De Paepe R, Cornic G, Streb P (2006a) The mitochondrial CMSII mutation of Nicotiana sylvestris impairs adjustment of photosynthetic carbon assimilation to higher growth irradiance. J Exp Bot 57: 2075-2085
Pubmed: Author and Title
CrossRef: Author and Title
Google Scholar: Author Only Title Only Author and Title

Priault P, Tcherkez G, Cornic G, De Paepe R, Naik R, Ghashghaie J,Streb P (2006b) The lack of mitochondrial complex I in a CMSII

mutant of Nicotiana sylvestris increases photorespiration through an increased internal resistance to CO2 diffusion. J Exp Bot 57: 3195-3207

Pubmed: Author and Title
CrossRef: Author and Title
Google Scholar: Author Only Title Only Author and Title

Priault P, Vidal G, De Paepe R, Ribas-Carbo M (2007) Leaf age-related changes in respiratory pathways are dependent on complex I activity in Nicotiana sylvestris. Physiol Plant 129: 152-162

Pubmed: Author and Title
CrossRef: Author and Title
Google Scholar: Author Only Title Only Author and Title

Price, T O, Eranki, V, Banks, W A, Ercal, N, Shah, G N (2011) Topiramate treatment protects blood-brain barrier pericytes from hyperglycemia-induced oxidative damage in diabetic mice. Endocrinology 153: 362-372

Pubmed: Author and Title
CrossRef: Author and Title
Google Scholar: Author Only Title Only Author and Title

Procaccio V, Wallace DC (2004) Late-onset Leigh syndrome in a patient with mitochondrial complex I NDUFS8 mutations. Neurology 62: 1899-1901

Pubmed: Author and Title
CrossRef: Author and Title
Google Scholar: Author Only Title Only Author and Title

Qin Y, Leydon AR, Manziello A, Pandey R, Mount D, Denic S, Vasic B, Johnson MA, Palanivelu R (2009) Penetration of the stigma and style elicits a novel transcriptome in pollen tubes, pointing to genes critical for growth in a pistil. PLoS Genet 5: e1000621

Pubmed: Author and Title
CrossRef: Author and Title
Google Scholar: Author Only Title Only Author and Title

Queval G, Issakidis-Bourguet E, Hoeberichts FA, Vandorpe M, Gakière B, Vanacker H, Miginiac-Maslow M, Van Breusegem F, Noctor G (2007a) Conditional oxidative stress responses in the Arabidopsis photorespiratory mutant cat2 demonstrate that redox state is a key modulator of daylength-dependent gene expression, and define photoperiod as a crucial factor in the regulation of H2O2-induced cell death. Plant J 52: 640-657

Pubmed: Author and Title
CrossRef: Author and Title
Google Scholar: Author Only Title Only Author and Title

Queval G, Neukermans J, Vanderauwera S, Van Breusegem F, Noctor G (2012) Day length is a key regulator of transcriptomic responses to both CO(2) and H(2)O(2) in Arabidopsis. Plant Cell Environ 35: 374-387

Pubmed: Author and Title
CrossRef: Author and Title
Google Scholar: Author Only Title Only Author and Title

Queval G, Noctor G (2007b) A plate reader method for the measurement of NAD, NADP, glutathione, and ascorbate in tissue extracts: application to redox profiling during Arabidopsis rosette development. Anal Biochem 363: 58-69

Pubmed: Author and Title
CrossRef: Author and Title
Google Scholar: Author Only Title Only Author and Title

Rasmusson AG, Geisler DA, Møller IM (2008) The multiplicity of dehydrogenases in the electron transport chain of plant mitochondria. Mitochondrion 8: 47-60

Pubmed: Author and Title
CrossRef: Author and Title
Google Scholar: Author Only Title Only Author and Title

Rasmusson AG, Wallström S V (2010) Involvement of mitochondria in the control of plant cell NAD (P) H reduction levels. Biochem Soc Trans 38:661-666

Pubmed: Author and Title
CrossRef: Author and Title
Google Scholar: Author Only Title Only Author and Title

Rey G, Reddy AB (2013) Protein acetylation links the circadian clock to mitochondrial function. Proc Natl Acad Sci U S A 110: 3210-3211

Pubmed: Author and Title
CrossRef: Author and Title
Google Scholar: Author Only Title Only Author and Title

Ribas-Carbo M, Berry JA, Yakir D, Giles L, Robinson SA, Lennon AM, Siedow JN (1995) Electron Partitioning between the Cytochrome and Alternative Pathways in Plant Mitochondria. Plant Physiol 109: 829-837

Pubmed: Author and Title
CrossRef: Author and Title
Google Scholar: Author Only Title Only Author and Title

Robbins NS, Pharr DM (1987) Regulation of photosynthetic carbon metabolism in cucumber by light intensity and photosynthetic period. Plant Physiol 85: 592-597

Pubmed: Author and Title
CrossRef: Author and Title
Google Scholar: Author Only Title Only Author and Title

Sabar M, De Paepe R, de Kouchkovsky Y (2000) Complex I impairment, respiratory compensations, and photosynthetic decrease in nuclear and mitochondrial male sterile mutants of Nicotiana sylvestris. Plant Physiol 124: 1239-1250

Pubmed: Author and Title
CrossRef: Author and Title
Google Scholar: Author Only Title Only Author and Title

Saisho D, Nambara E, Naito S, Tsutsumi N, Hirai A, Nakazono M (1997) Characterization of the gene family for alternative oxidase from Arabidopsis thaliana. Plant Mol Biol 35: 585-596

Pubmed: Author and Title
CrossRef: Author and Title
Google Scholar: Author Only Title Only Author and Title

Sassone-Corsi P (2012) Minireview: NAD+, a circadian metabolite with an epigenetic twist. Endocrinology 153: 1-5

Pubmed: Author and Title
CrossRef: Author and Title
Google Scholar: Author Only Title Only Author and Title

Schmid M, Davison TS, Henz SR, Pape UJ, Demar M, Vingron M, Schölkopf B, Weigel D, Lohmann JU (2005) A gene expression map of Arabidopsis thaliana development. Nat Genet 37: 501-506

Pubmed: Author and Title
CrossRef: Author and Title
Google Scholar: Author Only Title Only Author and Title

Schreiber V, Dantzer F, Ame J-C, de Murcia G (2006) Poly(ADP-ribose): novel functions for an old molecule. Nat Rev Mol Cell Biol 7: 517-528

Pubmed: Author and Title
CrossRef: Author and Title
Google Scholar: Author Only Title Only Author and Title

Seemann JR, Sharkey TD (1986) Salinity and Nitrogen Effects on Photosynthesis, Ribulose-1,5-Bisphosphate Carboxylase and Metabolite Pool Sizes in Phaseolus vulgaris L. Plant Physiol 82: 555-560

Pubmed: Author and Title
CrossRef: Author and Title
Google Scholar: Author Only Title Only Author and Title

Shah, J. K., Cochrane, D. W., De Paepe, R., & Igamberdiev, A. U. (2013). Respiratory complex I deficiency results in low nitric oxide levels, induction of hemoglobin and upregulation of fermentation pathways. Plant physiology and biochemistry, 63:185-190.

Pubmed: Author and Title
CrossRef: Author and Title
Google Scholar: Author Only Title Only Author and Title

Shen, W., Wei, Y., Dauk, M., Tan, Y., Taylor, D. C., Selvaraj, G., & Zou, J. (2006). Involvement of a glycerol-3-phosphate dehydrogenase in modulating the NADH/NAD+ ratio provides evidence of a mitochondrial glycerol-3-phosphate shuttle in Arabidopsis. The Plant Cell, 18: 422-441

Pubmed: Author and Title
CrossRef: Author and Title
Google Scholar: Author Only Title Only Author and Title

Shim JS, Imaizumi T (2015) Circadian clock and photoperiodic response in Arabidopsis: from seasonal flowering to redox homeostasis. Biochemistry (Mosc) 54: 157-170

Pubmed: Author and Title
CrossRef: Author and Title
Google Scholar: Author Only Title Only Author and Title

Smith CA, Want EJ, O'Maille G, Abagyan R, Siuzdak G (2006) XCMS: processing mass spectrometry data for metabolite profiling using nonlinear peak alignment, matching, and identification. Anal Chem 78: 779-787

Pubmed: Author and Title
CrossRef: Author and Title
Google Scholar: Author Only Title Only Author and Title

Soto D, Córdoba JP, Villarreal F, Bartoli C, Schmitz J, Maurino VG, Braun HP, Pagnussat GC, Zabaleta E (2015) Functional characterization of mutants affected in the carbonic anhydrase domain of the respiratory complex I in Arabidopsis thaliana. The Plant Journal 83: 831-844

Pubmed: Author and Title
CrossRef: Author and Title
Google Scholar: Author Only Title Only Author and Title

de Sousa CAF, Sodek, L (2002). The metabolic response of plants to oxygen deficiency. Brazilian Journal of Plant Physiology 14: 83-94

Pubmed: Author and Title
CrossRef: Author and Title
Google Scholar: Author Only Title Only Author and Title

Stangherlin A, Reddy AB (2013) Regulation of circadian clocks by redox homeostasis. J Biol Chem 288: 26505-26511

Pubmed: Author and Title
CrossRef: Author and Title
Google Scholar: Author Only Title Only Author and Title

Streb P, Feierabend J, Bligny R (1997) Resistance to photoinhibition of photosystem II and catalase and antioxidative protection in high mountain plants. Plant Cell Environ 20: 1030-1040

Sunderhaus S, Dudkina NV, Jänsch L, Klodmann J, Heinemeyer J, Perales M, Zabaleta E, Boekema EJ, Braun H-P (2006) Carbonic anhydrase subunits form a matrix-exposed domain attached to the membrane arm of mitochondrial complex I in plants. Journal of Biological Chemistry 281: 6482-6488

Sweetlove L J, Beard K F, Nunes-Nesi A, Fernie AR, Ratcliffe R G (2010) Not just a circle: flux modes in the plant TCA cycle. Trends in plant science, 15: 462-470

Szal B, Dabrowska Z, Malmberg G, Gardeström P, Rychter AM (2008) Changes in energy status of leaf cells as a consequence of mitochondrial genome rearrangement. Planta 227: 697-706

Tan B, Young DA, Lu Z-H, Wang T, Meier TI, Shepard RL, Roth K, Zhai Y, Huss K, Kuo M-S, et al (2013) Pharmacological inhibition of nicotinamide phosphoribosyltransferase (NAMPT), an enzyme essential for NAD+ biosynthesis, in human cancer cells: metabolic basis and potential clinical implications. J Biol Chem 288: 3500-3511

Tcherkez G, Mahe A, Gauthier P, Mauve C, Gout E, Bligny R, Cornic G, Hodges M (2009) In Folio Respiratory Fluxomics Revealed by 13C Isotopic Labeling and H/D Isotope Effects Highlight the Noncyclic Nature of the Tricarboxylic Acid "Cycle" in Illuminated Leaves. Plant Physiol 151: 620-630

Tcherkez G, Schäufele R, Nogués S, Piel C, Boom A, Lanigan G, Barbaroux C, Mata C, Elhani S, Hemming D, et al (2010) On the 13C/12C isotopic signal of day and night respiration at the mesocosm level. Plant Cell Environ 33: 900-913

Tomaz, T, Bagard M, Pracharoenwattana I, Lindén P, Lee CP, Carroll A J, ... & Millar A H (2010) Mitochondrial malate dehydrogenase lowers leaf respiration and alters photorespiration and plant growth in Arabidopsis. Plant Physiol 154: 1143-1157

Tschoep H, Gibon Y, Carillo P, Armengaud P, Szecowka M, Nunes-Nesi A, Fernie AR, Koehl K, Stitt M (2009) Adjustment of growth and central metabolism to a mild but sustained nitrogen-limitation in Arabidopsis. Plant Cell Environ 32: 300-318

Vanderauwera S, Zimmermann P, Rombauts S, Vandenabeele S, Langebartels C, Gruissem W, Inzé D, Van Breusegem F (2005) Genome-wide analysis of hydrogen peroxide-regulated gene expression in Arabidopsis reveals a high light-induced transcriptional cluster involved in anthocyanin biosynthesis. Plant Physiol 139: 806-821

Vanlerberghe, G. C., & McIntosh, L. (1996). Signals regulating the expression of the nuclear gene encoding alternative oxidase of plant mitochondria. Plant Physiology, 111: 589-595.

Verkaart S, Koopman WJH, van Emst-de Vries SE, Nijtmans LGJ, van den Heuvel LWPJ, Smeitink JAM, Willems PHGM (2007) Superoxide production is inversely related to complex I activity in inherited complex I deficiency. Biochim Biophys Acta 1772: 373-381

Vidal G, Ribas-Carbo M, Garmier M, Dubertret G, Rasmusson AG, Mathieu C, Foyer CH, De Paepe R (2007) Lack of respiratory chain complex I impairs alternative oxidase engagement and modulates redox signaling during elicitor-induced cell death in tobacco. Plant Cell 19: 640-655

Google Scholar: <u>Author Only</u> <u>Title Only</u> <u>Author and Title</u>

Vogel RO, Smeitink JAM, Nijtmans LGJ (2007) Human mitochondrial complex I assembly: a dynamic and versatile process. Biochim Biophys Acta 1767: 1215-1227

Pubmed: <u>Author and Title</u>
CrossRef: <u>Author and Title</u>
Google Scholar: <u>Author Only</u> <u>Title Only</u> <u>Author and Title</u>

Wallström SV, Florez-Sarasa I, Araújo WL, Aidemark M, Fernández-Fernández M, Fernie AR, Ribas-Carbó M, Rasmusson AG (2014) Suppression of the External Mitochondrial NADPH Dehydrogenase, NDB1, in Arabidopsis thaliana Affects Central Metabolism and Vegetative Growth. Mol Plant 7: 356-368

Pubmed: <u>Author and Title</u>
CrossRef: <u>Author and Title</u>
Google Scholar: <u>Author Only</u> <u>Title Only</u> <u>Author and Title</u>

Wang Q, Fristedt R, Yu X, Chen Z, Liu H, Lee Y, Guo H, Merchant SS, Lin C (2012) The ?-carbonic anhydrase subcomplex of mitochondrial complex I is essential for development and important for photomorphogenesis of Arabidopsis. Plant Physiol 160: 1373-1383

Pubmed: <u>Author and Title</u>
CrossRef: <u>Author and Title</u>
Google Scholar: <u>Author Only</u> <u>Title Only</u> <u>Author and Title</u>

Willekens H, Chamnongpol S, Davey M, Schraudner M, Langebartels C, Van Montagu M, Inzé D, Van Camp W (1997) Catalase is a sink for H2O2 and is indispensable for stress defence in C3 plants. EMBO J 16: 4806-4816

Pubmed: <u>Author and Title</u>
CrossRef: <u>Author and Title</u>
Google Scholar: <u>Author Only</u> <u>Title Only</u> <u>Author and Title</u>

Yoshida K, Noguchi K (2009) Differential gene expression profiles of the mitochondrial respiratory components in illuminated Arabidopsis leaves. Plant and Cell Physiology, 50: 1449-1462

Pubmed: <u>Author and Title</u>
CrossRef: <u>Author and Title</u>
Google Scholar: <u>Author Only</u> <u>Title Only</u> <u>Author and Title</u>

Yoshida K, Noguchi K (2009) Differential gene expression profiles of the mitochondrial respiratory components in illuminated Arabidopsis leaves. Plant and Cell Physiology, 50: 1449-1462

Pubmed: <u>Author and Title</u>
CrossRef: <u>Author and Title</u>
Google Scholar: <u>Author Only</u> <u>Title Only</u> <u>Author and Title</u>

Zabaleta E, Martin MV, Braun HP (2012) A basal carbon concentrating mechanism in plants? Plant Sci 187: 97-104

Pubmed: <u>Author and Title</u>
CrossRef: <u>Author and Title</u>
Google Scholar: <u>Author Only</u> <u>Title Only</u> <u>Author and Title</u>